Applied Geochemistry 209 (2026) 107053

Contents lists available at ScienceDirect

Applied Geochemistry

journal homepage: www.elsevier.com/locate/apgeochem

Baseline water quality and geochemistry of shallow groundwater used by indigenous communities in the vicinity of the Salar de Uyuni, Bolivia

Hannah Wudke, Gordon D.Z. Williams, Avner Vengosh *

Division of Earth and Climate Sciences, Nicholas School of the Environment, Duke University, Durham, NC, USA

ARTICLE INFO

Editorial handling by: Elisa Sacchi

ABSTRACT

One of the largest global known lithium brine resources is the Salar de Uyuni (SDU) in the Bolivian Altiplano, yet presently, lithium exploitation is limited. Large-scale lithium extraction could impact regional water resources, which are used by local indigenous communities. Here, we investigate the water quality and geochemistry of shallow groundwater in the vicinity of the SDU, evaluating geochemical factors that control the occurrence of geogenic contaminants. We present a suite of geochemical analyses of shallow groundwater (n = 63) used as a primarily drinking water source by communities surrounding the SDU. Integrated water quality data shows that concentrations levels in most groundwater exceeded the World Health Organization drinking water recommended threshold values for at least one contaminant. We show that salinity, arsenic, boron and lithium are the major geogenic constituents that pose risks to human health. These results are consistent with established patterns of geogenic water quality issues reported for other water resources in the high Andes. Our analysis shows that low salinity groundwater west of the SDU is characterized by low δ^2H and $\delta^{18}O$ with a slope that mimics the Local Meteoric Water Line and distinctively high boron, B/Li, Mg/Li, and low $^{87}Sr/^{86}Sr$, indicating water-rock interactions with associated andesitic rocks. Groundwater from the Rio Grande watershed and eastern of the SDU have higher δ^2H, $\delta^{18}O$, and $^{87}Sr/^{86}Sr$, reflecting local recharge and different lithological sources with a radiogenic Sr isotope composition. Through the region we identified hot spots of saline groundwater with low B/Li and Mg/Li ratios and with relatively low δ^2H and $\delta^{18}O$, as well as $^{87}Sr/^{86}Sr$ ratios that are different from those of the SDU brines, indicating rather mixing with underlying saline geothermal waters. Future large-scale lithium extraction could intensify groundwater pumping that would be likely to cause regional groundwater level drawdown and further increase the impact of underlying saline geothermal waters, exacerbating the already impaired quality of water resources for indigenous communities in the SDU vicinity.

1. Introduction

One of the major global water demands is allocating water for the energy sector along the different stages of energy production, including mining, processing, and distribution. The recent onset of the clean energy transition and accompanying large-scale extraction of critical minerals involves water intensive processes that pose additional strain on freshwater resources in areas of critical minerals mining (Liu and Agusdinata, 2020; Kirshen et al., 2025). In the Salar de Atacama in Chile lithium extraction induces large volumes of brine estimated as ~200 m^3 per ton of lithium carbonate equivalent (LCE) whereas the freshwater use for processing requires a volume of 25 m^3 per ton LCE (Palacios et al., 2026). Consequently, impacts have been shown in the Salar de Atacama, where large-scale Li extraction over the last three decades has resulted in drawdown of the groundwater table, which has triggered localized surface subsidence (Flexer et al., 2018; Marazuela et al., 2019, 2020; Bustos-Gallardo et al., 2021; Vera et al., 2023). The potential for critical mineral extraction to impact local water quality and/or availability highlights the ongoing need to sustainably manage limited groundwater resources and establish water quality baselines in regions hosting critical mineral deposits prior to large-scale extraction.

A critical mineral central to the clean energy transition is lithium (Li), a component of Li-ion batteries needed for energy storage and electric vehicles (International Energy Agency, 2021). Lithium is currently extracted from both hard-rock pegmatite deposits and closed-basin brines often found in salt flats ("salars") in South America

This article is part of a special issue entitled: Resource Environ Geochem published in Applied Geochemistry.

* Corresponding author.
E-mail address: vengosh@duke.edu (A. Vengosh).

https://doi.org/10.1016/j.apgeochem.2026.107053
Received 10 May 2026; Received in revised form 5 August 2026; Accepted 21 August 2026
Available online 28 August 2026

(Kesler et al., 2012; Jaskula, 2024). Salt flats form in continental closed-basins, where dilute inflows already enriched in Li are gradually concentrated by evaporative enrichment (Eugster and Hardie, 1978). Many of these salt flat systems were formed in the dry, high Central Andes in South America, constituting a region known as the Lithium Triangle, which is estimated to contain up to 60% of global Li reserves (Jaskula, 2024; Moon, 2024; Munk et al., 2025). The largest of these deposits is the Salar de Uyuni (SDU) in the Bolivian Altiplano (Fig. 1), with a surface area of 10,000 km^2 and an inferred resource of 19.2 Mt of Li (Risacher and Fritz, 1991a, 1991b; YLB, 2019). However, Li extraction in the SDU has not yet progressed beyond pilot scale extraction (Williams and Vengosh, 2025).

Although comprehensive hydrogeological data in the immediate proximity to the SDU is not available, pervasive water quality issues have been demonstrated in the Altiplano as a function of the geological setting and/or mining activities unrelated to Li mining (Risacher and Fritz, 1991b; Banks et al., 2004; Ormachea Muñoz et al., 2015; 2013; Lima et al., 2019, 2020; Tapia et al., 2019). In particular, arsenic (As), boron (B), Li and salinity have been reported as high levels, and As and B commonly exceed World Health Organization (WHO) drinking water recommended values in the local groundwater (Banks et al., 2004; Concha et al., 2010).

In the Altiplano region, the occurrence of geogenic As in groundwater has been attributed to weathering of volcanic rocks and leaching of silicic glasses (Murray et al., 2023), influx of geothermal fluids enriched with As (Banks et al., 2004; Morteani et al., 2014; Ormachea Muñoz et al., 2015; Morales-Simfors et al., 2020; Muller et al., 2020), and volcanism (Tapia et al., 2019; Morales-Simfors et al., 2020). In many of these cases, the basaltic rocks are enriched in As, which is then mobilized through water-rock interactions to the local groundwater (Murray et al., 2023). Similar to the observed behavior of As in shallow groundwaters globally, As in groundwater from the lower Katari Basin and southern Poopo Basin of the Bolivian Altiplano is commonly found as oxidized As(V) and more mobile under slightly alkaline conditions in sodium - bicarbonate (Na-HCO_3) type waters (Smedley and Kinniburgh, 2002; Ormachea Muñoz et al., 2013).

Boron and Li in natural waters of the Altiplano are also commonly attributed to volcanic and geothermal sources. In the southern Bolivian Altiplano, Risacher and Fritz (2009, 1991b) suggested B and Li content in cold spring waters resulted from alteration of andesitic volcanic rocks, brine recycling, and dissolution of evaporite deposits in the subsurface. Boron enrichment has been observed in geothermal waters of the Altiplano and is also linked to water-rock interactions with andesitic rocks (Kasemann et al., 2004; Morteani et al., 2014; Schmitt et al., 2002).

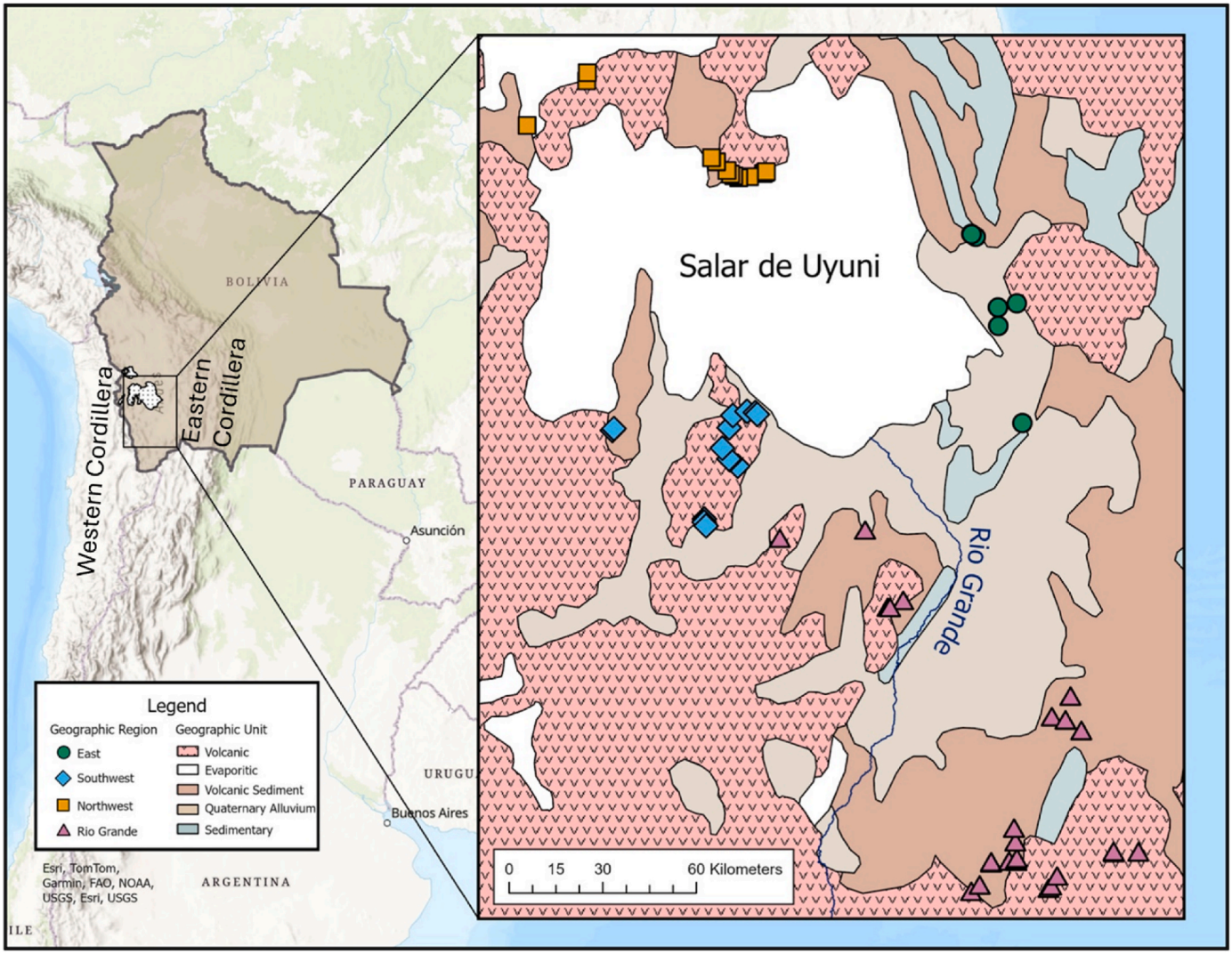

Fig. 1. General and geological maps with sample locations investigated in this study in the vicinity of the Salar de Uyuni, Bolivia. The northwest sampling group is represented by orange squares, the east by green circles, the southwest by blue diamonds, and the Rio Grande watershed by pink triangles. Note that the basin situated between the western and eastern mountain ranges (Cordillera Occidental and Cordillera Oriental) of the Central Andes. (For interpretation of the references to color in this figure legend, the reader is referred to the Web version of this article.)

Elsewhere, silicic volcanic rocks enriched in Li have been shown to leach Li during water-rock interaction, often resulting in economically valuable Li resources (Hofstra et al., 2013; Álvarez-Amado et al., 2022; Ellis et al., 2022; Cortes-Calderon et al., 2025; Del Bono et al., 2026). In similar closed-basin playa settings in Nevada, USA, geothermal waters were shown to be enriched in Li, where Li is leached at high temperatures and remains mobile during ascension to lower temperature groundwater (Araoka et al., 2014). Recent laboratory experiments on volcanic rocks from New Zealand has also suggested that Li leaching is significantly enhanced with increasing thermal water temperature (Sajkowski et al., 2025).

Here, we investigate the water quality and geochemistry of shallow groundwater in the vicinity of the SDU in Bolivia (Fig. 1). The local indigenous communities rely on shallow, untreated wells and surficial springs for drinking and agricultural water. The objective of this study is to evaluate the occurrence and distribution of geogenic contaminants through a systematic sampling of available water resources combined with utilization of geochemical and isotope tracers of oxygen, hydrogen, and strontium. As far as we are aware, this is the first water quality study of groundwater resources used by communities in the SDU region. We hypothesize that the combination of lithology and geochemistry of the shallow groundwater resources within the watershed of the SDU controls the water quality and that future groundwater extraction projected for large-scale lithium extraction could further impact water availability and quality in that region. This study aims to establish a water quality baseline of shallow groundwater in the vicinity of the SDU prior to large-scale Li extraction, assess the occurrence of geogenic contaminants, and evaluate the geochemical factors that control their occurrences in the shallow groundwater resources.

2. Methods

2.1. Geological background

The Bolivian Altiplano of the high Central Andes is a north-south oriented high plateau situated between the Cordillera Occidental (western mountain range) and Cordillera Oriental (eastern ridge) of the Central Andes. In the lower-lying salt flats of the Bolivian Altiplano, such as the SDU and the Salar de Coipasa (SDC), the mean elevation is ~3653 masl, whereas surrounding summits reach up to 6000 masl.

The Cordillera Occidental is an active volcanic arc generated by subduction located west of the SDU. The range is dominantly composed of andesites and dacites of Late Miocene and Quaternary age, as well as associated ignimbrite and tuff deposits. These volcanic deposits overlie Tertiary clastic and evaporite deposits. The Cordillera Oriental range to the east is a highly fractured fold and thrust belt of Paleozoic and Mesozoic marine shales and sandstones, which overlies a Precambrian basement. The range is cut by intrusive rocks of Paleozoic and Miocene age and is overlain in some regions by ignimbrites. The southeastern region of the SDU is characterized by abundant Quaternary sedimentary alluvium and evaporite deposits.

The western cordillera and Bolivian Altiplano comprise a portion of the Central Volcanic Zone (CVZ), which is one of the largest ignimbrite provinces globally (Stern, 2004). The eruptive history is dominated by eruptions of andesitic to dacitic composition, including lava flows, ignimbrites, and pyroclastics (Schnurr et al., 2007). Geophysical evidence indicates the presence of a large magmatic body and high heat flow beneath the southern Altiplano (de Silva et al., 2006). Thermal springs are abundant regionally, and near the eastern cordillera in the lake Poopó basin, they are associated with deep fault zones, where hot waters readily ascend to the surface through fractures (Ormachea Muñoz et al., 2015).

The SDU and SDC, situated between the two Cordilleras (Fig. 1), are remnants of several large paleolakes that occupied the southern Altiplano during the Pleistocene, the most recent of which desiccated as recently as ~11 thousand years ago (Baker et al., 2001; Fornari et al., 2001; Placzek et al., 2013; Risacher and Fritz, 1991a, 1991b). The combined effect of an arid climate, closed-basin tectonic setting, abundance of solutes, and a suitable timescale for evapoconcentration, are key factors leading to the formations of salt flats, such as the SDU (Munk et al., 2025; Williams et al., 2026).

2.2. Field sampling

Water samples were collected during a single campaign in September 2024. Locations of water samples (n = 63) sorted by their location with respect to the SDU are depicted in Fig. 1. Water sampling coordination and collection were conducted after getting the permission of the local indigenous organization, Federación Regional Única de Trabajadores Campesinos del Altiplano Sur (FRUTCAS). Individual sampling locations were primarily guided by community members and included water sources that are used as drinking water and/or for irrigation. Individual samples and communities were grouped into four subregions (east, northwest, southwest, and Rio Grande) based on their geographic location with respect to SDU (Fig. 1). These groupings are partially based on general physiographic/geologic variations and are used for geospatial and statistical analyses. All the samples in the northwest and southwest regions were collected from lithology primarily composed of andesitic or rhyolitic volcanic rocks, the Rio Grande region composed of Quaternary alluvium and andesitic or rhyolitic volcanic rocks, and the east lithology was composed of sedimentary rocks (Fig. 1).

pH, electrical conductivity (EC), and dissolved oxygen (DO) were measured in the field, using a Hanna HI98494 multiparameter probe calibrated daily. All water samples were extracted and filtered (0.45 μm) with a syringe filter in the field. Samples for alkalinity were filtered into clean high-density polyethylene (HDPE) bottles that were triple rinsed on site and filled without headspace. Samples for cations and trace elements were filtered into acid-washed HDPE bottles and acidified to pH < 2 with Fisher brand optima HNO_3^-. Samples for strontium isotopes and anions were filtered into clean HDPE bottles. More detailed descriptions of sample collection methods are available elsewhere (Williams et al., 2025a, 2025b; Williams and Vengosh, 2025). All data collected for each sample is in Table S1.

Water sample included surficial springs (n = 45), shallow wells (n = 11), streams (n = 3), a river (n = 1), a lake (n = 1), and tap water samples (n = 2) provided by the community members, which are indicated hereafter as groundwater owing to their original source from community wells. All samples were classified into broader groups, as either low salinity groundwater (n = 52), where TDS < 1000 mg/L, surface waters (n = 5), or saline groundwater (n = 6) in which TDS > 1000 mg/L. Finally, data for geothermal water from the region are from Morteani et al. (2014), Muller et al. (2020), and Ormachea Muñoz et al. (2015) are tabulated in Table S2. SDU brine chemistry data are from Williams et al. (2026) and rock geochemistry data are from Muller et al. (2020) and available in Table S3 and Table S4, respectively.

2.3. Water analysis

Major ions were measured with ion chromatography (IC) at Duke University. Cation (Na^+, K^+, Mg^{2+}, Ca^{2+}) concentrations were measured on a Thermo Scientific Aquion IC, and anion (F^-, Cl^-, Br^-, NO_3^{2-}, SO_4^{2-}) concentrations were measured on a Thermo Scientific Dionex IC DX-2100. Trace elements were measured at Duke University with a Thermo Fischer X-Series II Inductively-Coupled Plasma Mass Spectrometer (ICP-MS). Randomly selected replicates and DI water (>18 MΩ/cm) blanks were regularly included. Total alkalinity, expressed as [HCO_3^-], was determined by titration with 0.02 N HCl on a Metrohm Eco Autotitrator (Williams et al., 2025b). Reaction errors for all samples were less than ±5%. For strontium (Sr) isotope analysis ($^{87}Sr/^{86}Sr$), Sr was purified with Sr-spec resin (Eichrom) and HNO_3 (Hall et al., 2025; Hill et al., 2025). For all analyses, accuracy was verified by regularly running the IAPSO Atlantic seawater standard and waters from

the USGS Standard Reference Sample Project. Strontium isotopes were measured on a ThermoFisher Triton thermal ionization mass spectrometer (TIMS) at Duke University following standard procedures (Hall et al., 2025). NIST SRM-987 standards were measured repeatedly, yielding a long-term average of 0.710244 ± 0.000013 (n = 12); aligning with expected values (Jochum et al., 2005; McArthur et al., 2025); the IAPSO Atlantic seawater standard was also run yielding a value of 0.709166 ± 0.000009 (n = 10) also in agreement with expected values (Krabbenhöft et al., 2009). Strontium isotopic compositions are reported as both $^{87}Sr/^{86}Sr$ ratios and delta values ($\delta^{87}Sr$), where the long-term average of NIST SRM-987 in our analytical runs, yielding a reproducibility of ±0.02‰, was chosen for the standard in delta notation as shown in Equation (1):

$$\delta^{87}Sr\ (‰) = \frac{\left({}^{87}Sr/{}^{86}Sr_{\ sample} - {}^{87}Sr/{}^{86}Sr_{\ NIST\ 987} \right)}{{}^{87}Sr/{}^{86}Sr_{NIST\ 987}} \times 1000 \quad (1)$$

Oxygen and hydrogen isotopes were measured at the University of California, Davis stable isotope facility by headspace equilibrium with CO_2-He and H_2-He gas for O and H respectively. Oxygen isotopes in headspace CO_2 were measured on a Thermo Scientific GasBench II coupled to a Thermo Finnigan Delta Plus XL IRMS and H isotopes in headspace H_2 were measured on a Thermo Scientific GasBench II coupled to a Thermo Electron Delta V Plus IRMS. Replicate analysis of reference materials for O and H across the mass range yield a precision of ±0.04‰ for $\delta^{18}O$ and of ±1.1‰ for $\delta^{2}H$ referenced to VSMOW.

2.4. Data analysis

All statistical analyses were performed with R (version 4.4.3) (R Core Team, 2023). Spearman's Rank Correlation (Spearman's Rho, ρ) was chosen as the nonparametric measurement of the strength between two variables in waters. Statistical significance of the Spearman's Rho values is evaluated with p values, where a 99% confidence interval is given when $p < 0.01$, and a 95% confidence interval is given when $p < 0.05$. Geospatial analyses were conducted on ArcGIS Pro (Version 3.5).

The redox speciation of arsenic as either As(III) or As(V) was simulated using the Specific ion Interaction Theory (SIT theory) database in PHREEQC (version 3.7.3). The pe of the solution was calculated using the Nernst equation with field measurements of the solution oxidation reduction potential (ORP) and temperatures. ORP measurements were performed on the same multiparameter probe with an Ag/AgCl (3 M KCl) reference electrode. The field measured potentials were converted to the standard hydrogen electrode (SHE) scale by adding 0.22 V O_2 concentrations were adjusted to equilibrate the PHREEQC simulated pe to the field measured value of the solution. As dissolved oxygen concentrations were relatively high, the required adjustment produced small changes in the overall aqueous solution composition.

Mixing modeling of the groundwater was conducted through selecting the highest saline geothermal water in Pastos Grandes reported by Muller et al. (2020) as the saline endmember and two low-saline groundwater with slightly different chemical composition to represent the low-salinity endmember, generating two mixing modeling scenarios. The mixing modeling was conducted using the common mixing equations assuming all elements are conservative without modification by water-rock interactions.

3. Results

3.1. Major chemistry and trace elements variations

Results of field measurements (pH, temperature, conductivity, etc.) and major ion concentrations (Na, K, Mg, Ca, F, Cl, Br, NO_3, SO_4, HCO_3) are presented in Table S1, respectively. Most of the water samples had circumneutral pH range (median of 7.6) and were weakly oxidizing (median ORP of 26.9 mV). The only detected reducing waters samples were a saline spring in the northwest near the SDU (−18.5 mV), a saline spring in the southwest (−121.6 mV), a drinking water well in the southwest (−9.4 mV), and a spring in the Rio Grande area (−11.9 mV). In all waters, the groundwater salinity varies from low salinity (TDS of 354 mg/L) up to saline groundwater (4727 mg/L), with two exceptionally high salinity waters in the northwestern area.

The variations of Ca, Mg, SO_4, and HCO_3 versus chloride concentrations in (shown in mmol/L) are presented in Fig. 2. The chemistry is highly variable across the water types, with relatively high Ca, Mg, SO_4 and HCO_3 in a fraction of groundwater samples from the Rio Grande watershed as well as the saline groundwater from the eastern region (Fig. 2). Considering variations in the Na/Cl molar ratios, low-saline and saline groundwater from the northwest and southwest have Na/Cl ~1 whereas those from the east show Na/Cl typically greater than 1 with values around 1.3 (Fig. 2). The variations of the Ca/Cl, Mg/Cl, and SO_4/Cl (molar) ratios versus the TDS (Fig. 3) show that low salinity groundwater from the Rio Grande area has distinctively high Ca/Cl, Mg/Cl, and SO_4/Cl ratios, whereas the saline groundwater samples in all different geographic regions are characterized by consistently lower ratios. The groundwater from the Rio Grande region with relatively higher Ca and SO_4 have Ca/SO_4 ratios ~1, whereas the eastern groundwater has $Ca/SO_4 < 1$ (Fig. 3).

Arsenic concentrations ranged from 0.9 μg/L to 118.3 μg/L and exceeded the WHO recommended limit of 10 μg/L in 51% of sampled waters (n = 32), in which the median regional concentrations of 5.1 μg/L was detected in the northwest (n = 14), 12.3 μg/L in the southwest (n = 13), 11.8 μg/L in the Rio Grande (n = 25), and 15.6 μg/L in the east (n = 6) (Fig. 4, S1). Across the entire study area and within water types, As was not correlated with ORP or pH (Table S5). In all the regions except for the east, As was strongly positively correlated with F ($\rho = 0.58$, $p < 0.05$; Table S5). Arsenic was positively correlated with SO_4 in the northwest ($\rho = 0.58$, $p < 0.05$) and Rio Grande ($\rho = 0.61$, $p < 0.01$) regions. Arsenic was also strongly and positively correlated to Na in the southwest ($\rho = 0.70$, $p < 0.05$) and Rio Grande ($\rho = 0.60$, $p < 0.01$) and was correlated to HCO_3 ($\rho = 0.66$, $p < 0.01$) and Ca ($\rho = 0.66$, $p < 0.01$) in the Rio Grande region (Table S5).

Boron concentrations exhibited a wide range of concentrations across multiple orders of magnitude, from 100 μg/L to 10,200 μg/L. In 43% (n = 27) of all sampled waters, B exceeded the WHO recommended limit of 2400 μg/L. The median B concentration was 5600 μg/L in the northwest (n = 14), 2300 μg/L in the southwest (n = 13), 3400 μg/L in the east (n = 6), and much lower concentrations of 300 μg/L in the Rio Grande watershed (n = 25) (Fig. 4; Fig. S2). Boron content was exceptionally elevated in the northwest in groundwater associated with volcanic rocks of the western Cordillera. Boron contents ranged from 1600 μg/L in low salinity groundwaters, to surface waters (3900 μg/L), up to high salinity groundwater (6500 μg/L). In groundwater from all the regions, B followed a positive trend with Cl ($\rho = 0.89$, $p < 0.001$) and overall TDS ($\rho = 0.72$, $p < 0.01$), except for within a subset of the northwest groundwater, where in some low salinity groundwater the B concentrations were high without a correspondent increase in salinity (Fig. S3; Table S6).

Lithium concentrations in the studied groundwater also showed a wide range of 3.2 μg/L to 6700 μg/L. In all groundwater samples from all subregions, Li was strongly positively correlated to Cl ($\rho = 0.87$, $p < 0.01$; Fig. S4; Table S7). Lithium content generally increases from south to north, with median values of 12.5 μg/L in the Rio Grande (n = 25), 36.8 μg/L in the southwest (n = 13), 117 μg/L in the northwest (n = 14), and 167.8 μg/L in the east (n = 6) (Fig. 4; Fig. S5). Low salinity groundwater had a range of 3.2 - 709.3 μg/L, whereas Li concentrations in saline groundwater was from 1278 μg/L to 6723 μg/L.

To assess the potential health risks of co-exposures to contaminants in drinking water used by the local communities, we used the Integrated Water Quality (IWQ) parameter, based on that of Horton (1965) that was calculated as the sum of Cl, As, and B normalized to their respective

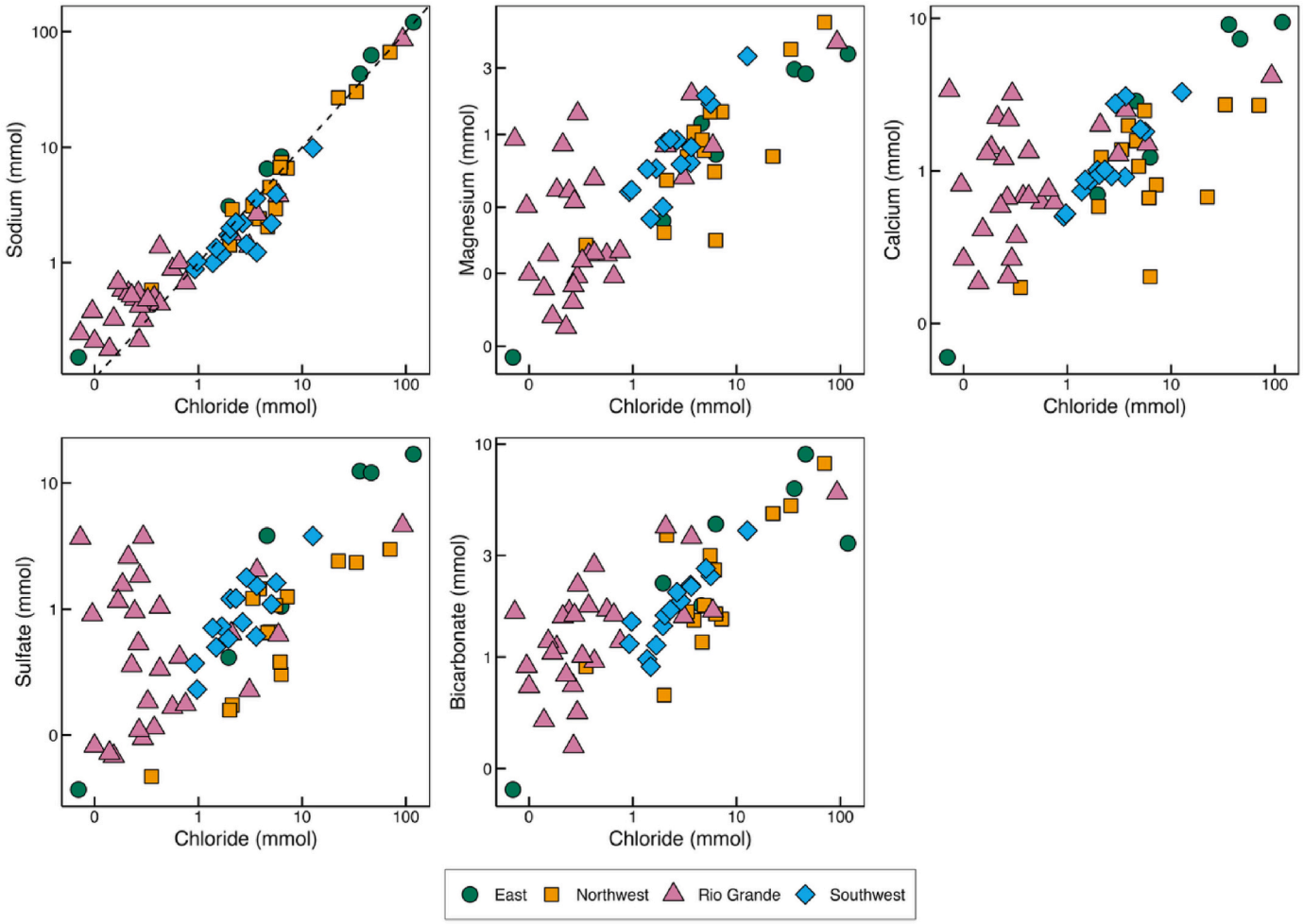

Fig. 2. Variations of Na, Ca, Mg, SO_4, and HCO_3 versus Cl in the investigated water samples, sorted by their geographical locations. The dashed black line represents a Na/Cl molar ratio of 1. Correlation coefficients are as follows: $\rho = 0.94$, $p < 0.001$ for Cl vs. Na; $\rho = 0.67$, $p < 0.001$ for Cl vs. Mg; $\rho = 0.41$, $p < 0.001$ for Cl vs. Ca; $\rho = 0.41$, $p < 0.001$ for Cl vs. SO_4; $\rho = 0.73$, $p < 0.001$ for Cl vs. bicarbonate (alkalinity).

WHO and EPA drinking water recommendations, as shown in Equation (2):

$$IWQ = \frac{\left(Chloride\ \left(\frac{mg}{L}\right)\right)}{250} + \frac{\left(Arsenic\ \left(\frac{ug}{L}\right)\right)}{10} + \frac{\left(Boron\ \left(\frac{ug}{L}\right)\right)}{2400} \quad (2)$$

IWQ has extensively used in the literature to evaluate the combination of water quality parameters and typically has been classified into 5 categories of excellent (<1), good (1–2), marginal (2–3), poor (3–5) and unsuitable (>5) and depends on the concentration of multiple contaminants present in groundwater samples (Mukate et al., 2019). Thus, higher IWQ indicates enrichment in one or more of these parameters above the recommended WHO threshold water quality parameters, and therefore less desirable water quality. In all studied waters, IWQ exhibits a wide range of 0.3 – 51.3. The median IWQ is variable across the study area, with 3.8 in the northwest, 2.8 in the southwest, 5.6 in the east, and 1.5 in the Rio Grande (Fig. 5). Water quality decreases from low salinity groundwater (median IWQ: 2.4) to saline groundwater (median IWQ: 9.1).

3.2. Boron and lithium occurrences

As part of this study, we evaluated the occurrences and relationships between Mg, B and Li in groundwater. B/Li molar ratios in groundwaters were highly variable (range 1 - 366). The highest B/Li ratios tend to occur in low salinity groundwater in the northwest (median: 33) and southwest (median: 49) regions, whereas low salinity groundwater from the Rio Grande region had intermediate ratios (median: 18). In contrast, saline groundwater from all regions shows systematically low B/Li ratios (~1.3). The B/Li ratios were strongly and negatively corrected with salinity in the northwest ($\rho = -0.85$, $p < 0.01$), southwest ($\rho = -0.65$, $p < 0.01$), and east ($\rho = -0.94$, $p < 0.01$), and a moderate negative correlation in the Rio Grande area ($\rho = -0.53$, $p < 0.01$) (Fig. 6). Similarly, our data show relatively high Mg/Li ratios in the low salinity groundwater, while saline groundwater had low Mg/Li ratios (Fig. 6).

In the northwest region, groundwater samples with elevated B/Li ratios (B/Li > 50) had a strong positive correlation between B/Li and Na/Cl ($\rho = 0.95$, $p < 0.01$; Fig. S6). In the same region, low B/Li waters with high salinity fall into two discrete groups. Near the Tahua community, on the northern edge of the SDU, 4 samples with low B/Li (<20) had high salinity compared to the region (TDS range of 531-5264 mg/L) and lower Na/Cl ratios (~0.9). Near Tres Cruces and the SDC, 3 samples with low B/Li ratios also had high salinity (TDS range of 551-2007 mg/L) and slightly elevated Na/Cl ratios (~1.2). In groundwater with high B/Li elsewhere across the SDU no correlation with Na/Cl were detected. Although As content did not demonstrate any obvious geospatial patterns, As content was inversely correlated with B/Li in the southwest ($\rho = -0.67$, $p < 0.01$), and the Rio Grande ($\rho = -0.40$, $p < 0.05$) regions (Fig. S7). Fluoride mimics this trend in both regions ($\rho = -0.63$, $p < 0.01$ and $\rho = -0.62$, $p < 0.01$, respectively) (Table S5), indicating that saline waters across the region share consistent geochemical composition of high F and As and low B/Li ratios.

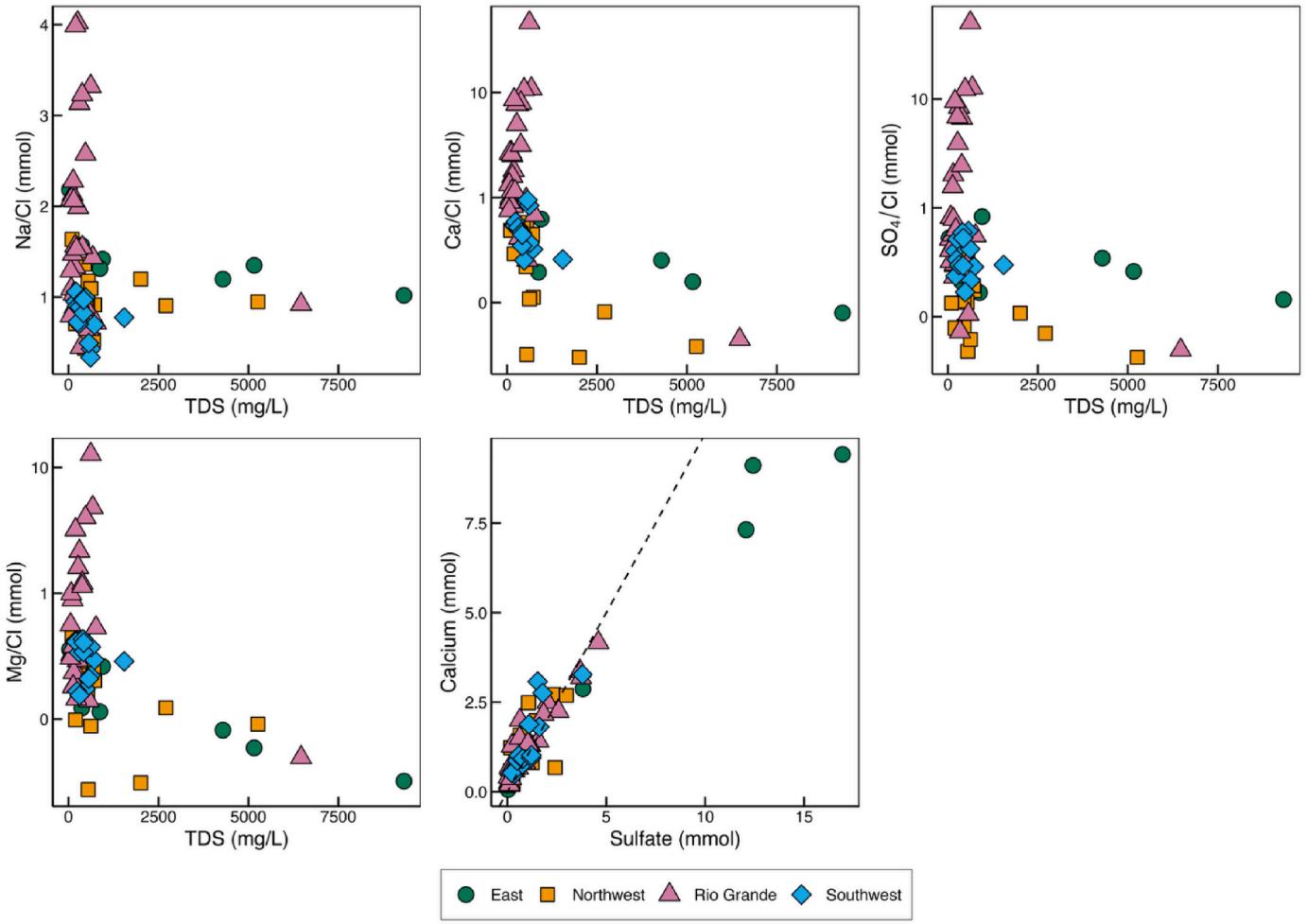

Fig. 3. Variations of Na/Cl, Ca/Cl, Mg/Cl and SO_4/Cl molar ratios versus TDS (mg/L) and Ca versus SO_4 (molar units) in the investigated water samples, sorted by their geographical locations. The dashed black line represents a Ca/SO_4 molar ratio of 1.

3.3. Strontium isotope geochemistry

Strontium concentrations (μg/L) and isotope ratios ($^{87}Sr/^{86}Sr$; $\delta^{87}Sr$) are reported in Table S9. Across all groundwater in the vicinity of the SDU, $\delta^{87}Sr$ showed a wide range from −6.3 ‰ to 2.6 ‰ ($^{87}Sr/^{86}Sr$ range = 0.7058 to 0.7121, Fig. S10). In the western area Sr isotope ratios were low (median $\delta^{87}Sr = -5.2$ ‰; $^{87}Sr/^{86}Sr = 0.7066$ in the southwest; and median $\delta^{87}Sr = -5.0$ ‰; $^{87}Sr/^{86}Sr$ median = 0.7067 in the northwest), while the ratios in the eastern groundwater were relatively high (median $\delta^{87}Sr = 0.8$ ‰; $^{87}Sr/^{86}Sr = 0.7108$). Groundwater from the Rio Grande watershed, which span a larger geographic area and contain regions that drain both the eastern and western Cordilleras, had variable isotope ratios with a $\delta^{87}Sr$ range of −4.3 ‰ to 2.3 ‰ ($^{87}Sr/^{86}Sr$ range = 0.7072 - 0.7118) (Fig. 7). The Sr isotope variations in groundwater detected in this study are consistent with the isotope variations previously reported for the local surface waters in catchments draining the eastern and western cordilleras of the Altiplano (Grove et al., 2003; Placzek et al., 2011), as well as the brines at the different sides of the SDU (Williams et al., 2025b). Placzek et al. (2011) have shown that the $^{87}Sr/^{86}Sr$ ratios of surface waters in catchments draining the eastern and western cordilleras surrounding the SDU have distinctive 0.7110 and 0.7069 ratios, respectively consistent with the results we report from shallow groundwater from these areas.

Notably, B/Li molar ratios were inversely correlated to $^{87}Sr/^{86}Sr$ in groundwater from the northwestern ($\rho = -0.55$, $p < 0.05$) and southwestern ($\rho = -0.57$, $p < 0.05$) regions (Fig. S8). However, no such correlations were detected in the eastern groundwater, or further south in the Rio Grande watershed. In the northwestern groundwater, Li content was positively correlated with $^{87}Sr/^{86}Sr$ ($\rho = 0.55$, $p < 0.05$) (Table S7), consistent with the inverse correlation of $^{87}Sr/^{86}Sr$ and B/Li ratios. In the Rio Grande basin, B was negatively correlated to $^{87}Sr/^{86}Sr$ ($\rho = -0.57$, $p < 0.01$) (Table S6). Arsenic was not related to $^{87}Sr/^{86}Sr$ in groundwater of any region (Table S5).

3.4. Stable isotopes of oxygen and hydrogen

Stable isotope data of oxygen ($\delta^{18}O$) and hydrogen ($\delta^{2}H$) are reported in Table S9. Across all groundwater in the vicinity of the SDU, $\delta^{18}O$ and $\delta^{2}H$ show large variations, and yet most of the $\delta^{18}O$ and $\delta^{2}H$ data of the groundwater are highly correlated and are associated with the Local Meteoric Water Line (LMWL) defined for modern precipitation in the Chilean and Bolivian Altiplano at altitudes of 2800–5700 m ($\delta^{2}H = 8.15 \times \delta^{18}O + 15.3$ (Chaffaut et al., 1998);) (Fig. 8). Groundwater from the northwestern and southwestern areas are characterized by relatively low $\delta^{18}O$ (median values of −16.6‰ and −15.5‰, respectively) and $\delta^{2}H$ (median values of −118.9‰ and −113.7‰, respectively), while groundwater from the Rio Grande watershed show systematically higher $\delta^{18}O$ (median values of −12.5‰) and $\delta^{2}H$ (median values of −91.3‰). Groundwater from the eastern area show overall low $\delta^{18}O$ (median values of −15.0‰) and $\delta^{2}H$ (median values of −115.3‰). A few saline groundwater samples deviate from the LMWL towards higher $\delta^{18}O$ (Fig. 8). Note the large distinction between the $\delta^{18}O$ and $\delta^{2}H$ values of the shallow groundwater with lower values and a $\delta^{2}H$-$\delta^{18}O$ slope of ~8 relative to shallow brines in the SDU with much higher

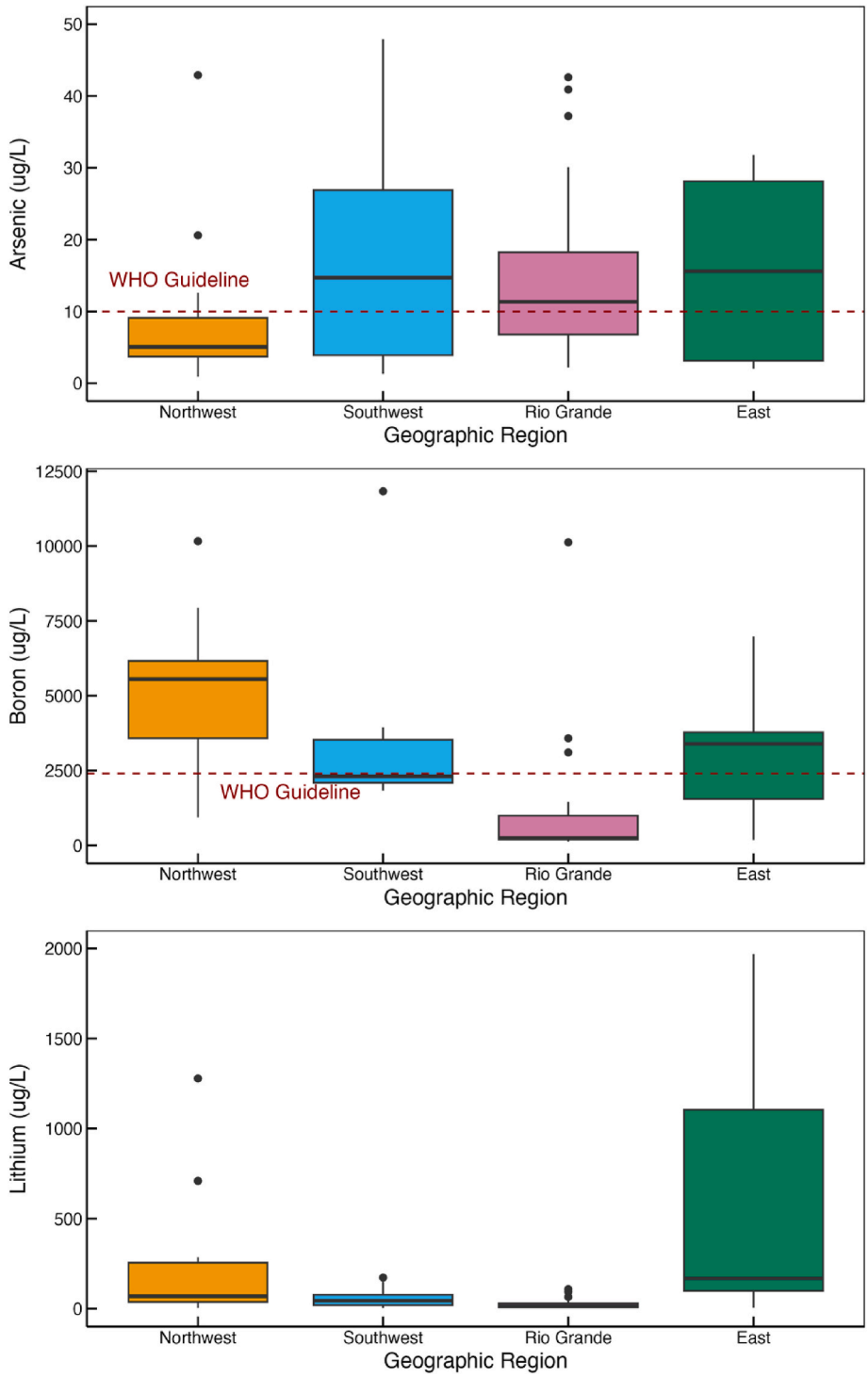

Fig. 4. *Boxplots of arsenic (μg/L), boron (μg/L), and lithium (μg/L) in groundwater from the northwest (orange), southwest (blue), Rio Grande (pink), and east (green) regions. Horizontal red dashed lines represent the WHO drinking water guidelines for arsenic and boron.* (For interpretation of the references to color in this figure legend, the reader is referred to the Web version of this article.)

values and a δ^2H-$\delta^{18}O$ evaporative slope of ~6.1 (Fig. 8) (Williams et al., 2026).

4. Discussion

4.1. Tracing the sources of the low-salinity groundwater

The variations in major elements composition of the investigated groundwater suggests that elemental mobilization from water-rock interactions directly affect the chemical composition of groundwater. The relatively low salinity and composition of groundwater associated with andesitic and dacitic rocks from the northwest and southwest regions (Fig. 1) are typical of local volcanic rocks alteration, specifically resulting in systematic Na/Cl ratios ~1 (Fig. 2) (Risacher and Fritz, 1991b, 2009). In contrast, low salinity groundwater from the Rio Grande region had elevated Ca and SO_4 with conspicuously high SO_4/Cl and Ca/Cl ratios, as well as Ca/SO_4 molar ratios of ~1, indicating interactions with rocks containing gypsum. This suggests that this

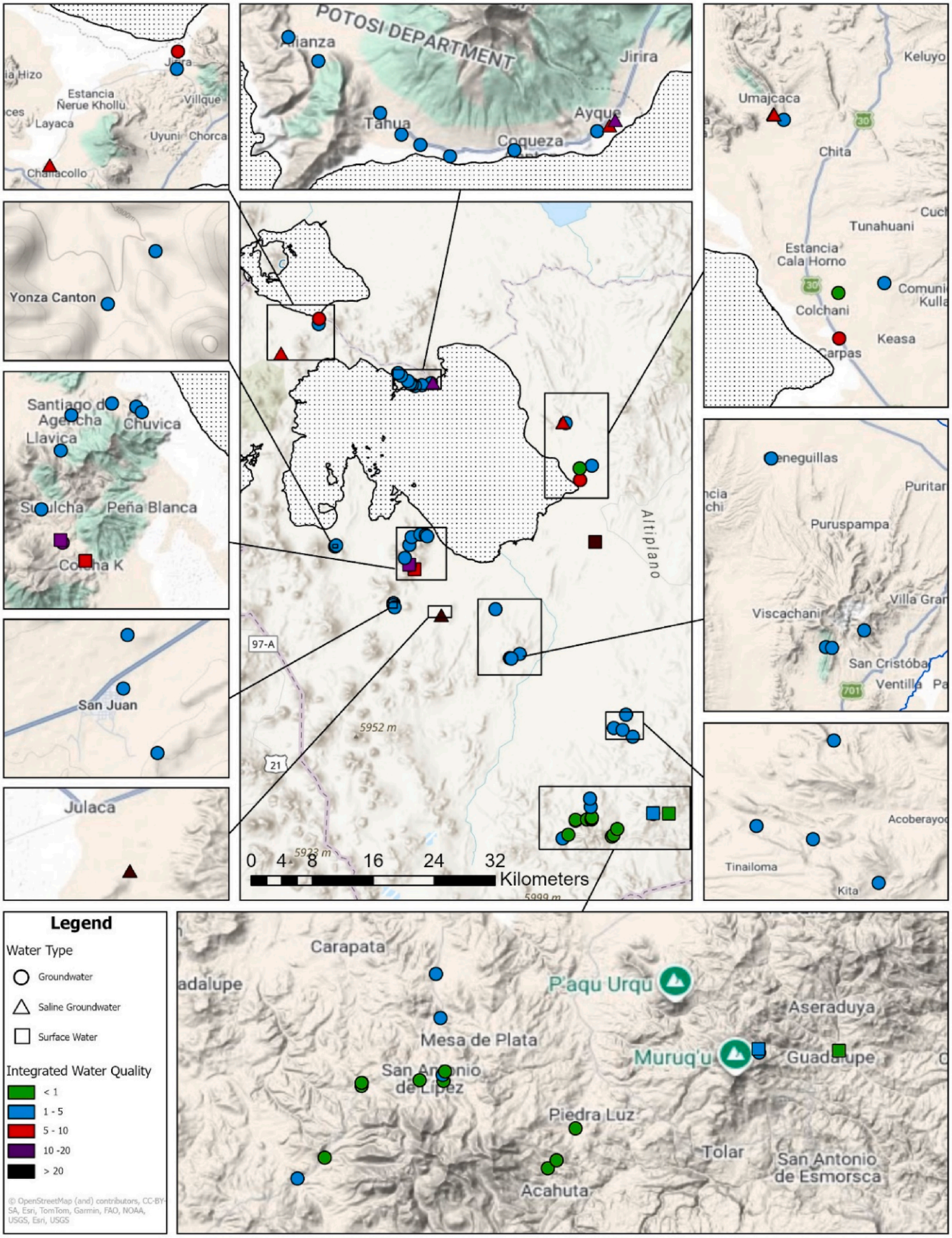

Fig. 5. Map depicting the spatial distribution of integrated water quality (IWQ) in low salinity groundwater (circles), high salinity groundwater (triangles), and surface water (squares). IWQ of less than 1 is green, from 1 to 5 is blue, from 5 to 10 is red, from 10 to 20 is purple, and greater than 20 is black, reflecting the severity of the water quality status. (For interpretation of the references to color in this figure legend, the reader is referred to the Web version of this article.)

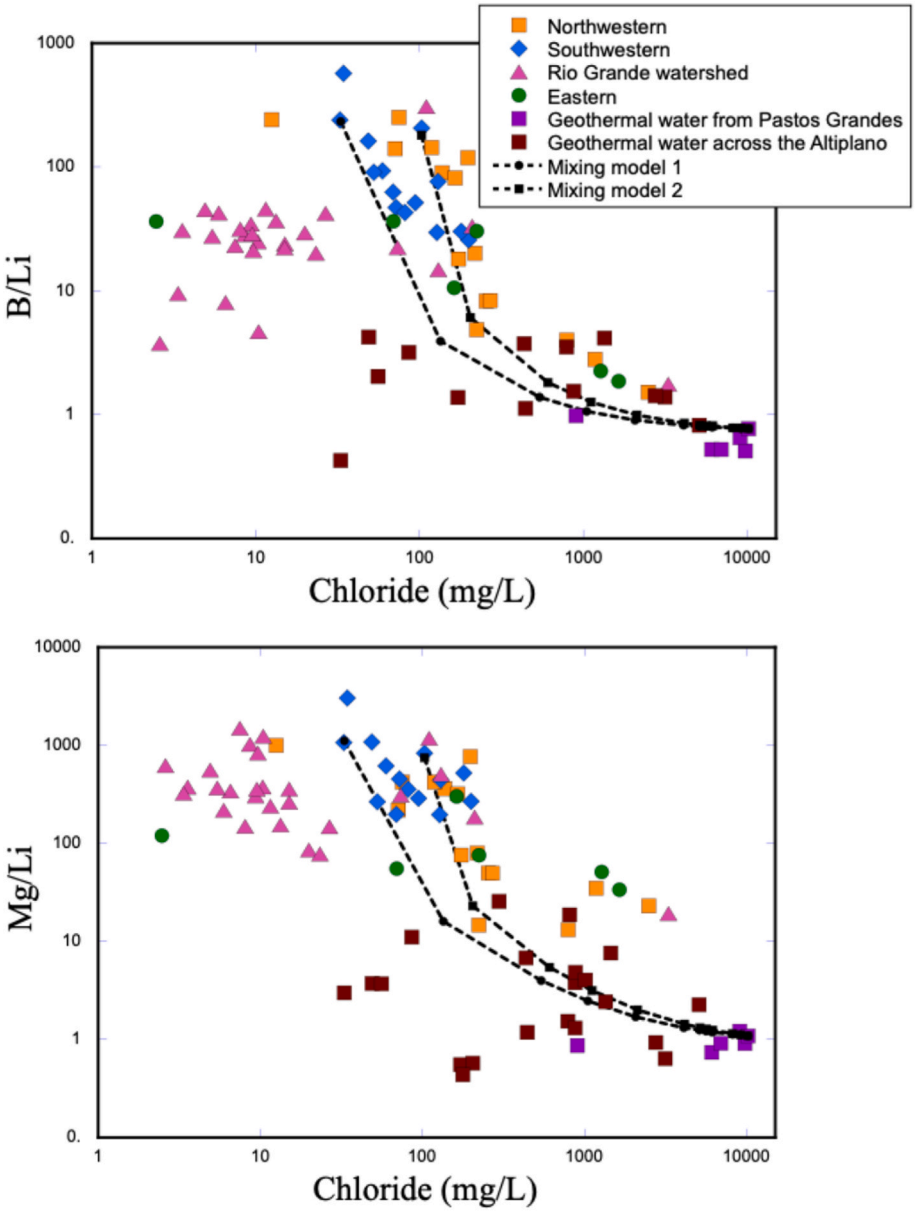

Fig. 6. B/Li and Mg/Li versus chloride (mg/L) in shallow groundwater surrounding the SDU in comparison to geothermal water from Pastos Grandes located south of the SDU (data from Muller et al., 2020) and geothermal water across the Altiplano (Morteani et al., 2014; Ormachea Muñoz et al., 2015). Note the potential mixing lines between the most saline geothermal water from Pastos Grandes and two low-salinity groundwater endmembers calculated in a mixing model conducted in this study (dashed lines).

subgroup of groundwater samples in the Rio Grande watershed is impacted by dissolution of local gypsum diapirs. Although the precise location of these evaporite deposits and gypsum diapirs is not available, they have been previously documented in the vicinity of the SDU region as a potential source of salinity for waters (Risacher and Fritz, 1991a, 2000). Groundwater from the eastern side of the SDU is associated with mixed lithologies of sedimentary and volcanic rocks and has relatively higher salinity and lower Na/Cl of 1.3 (Fig. 2), inferring a different source. The different lithology sources are clearly shown by the large differences in the $^{87}Sr/^{86}Sr$ ratios of groundwater from the west with low $^{87}Sr/^{86}Sr$ ratios which mimic the composition of the western Cordilleras volcanic (andesitic to dacitic) rocks as opposed to the eastern groundwater with higher $^{87}Sr/^{86}Sr$ ratios that are associated with the mixed sedimentary and volcanic lithology of the eastern Cordilleras. Such a distinction has been reported by Grove et al. (2003) and Placzek et al. (2011). Groundwater from the Rio Grande watershed shows intermediate $^{87}Sr/^{86}Sr$ ratios (Fig. 7) that likely reflects contributions from both the western and eastern Cordilleras rocks.

Our data reveal high B/Li and Mg/Li ratios in the low salinity groundwater, particularly in the northwest and southwest regions (Fig. S9). Williams and Vengosh (2026) have shown that Mg/Li ratios in low-temperature ($<30^{O}C$) and near-surface springs in the Lithium Triangle are characterized by relatively high Mg/Li ratios (median value = 31) that are consistent with the relatively high Mg/Li ratios reported in local rocks (i.e. ignimbrites, lavas, and some intrusive rocks) ranging from ~68 to 1050 (rock data from Mamani et al. (2010)). Consequently, the relatively high Mg/Li ratios in the low salinity groundwaters from the northwest (median = 80) and southwest (449) are consistent with this observation, indicating that low-temperature water-rock interactions induce similar mobilization of Mg and Li from the regional volcanic rocks, maintaining the relatively high Mg/Li ratios of the local lithologies. This evaluation is supported by the temperature

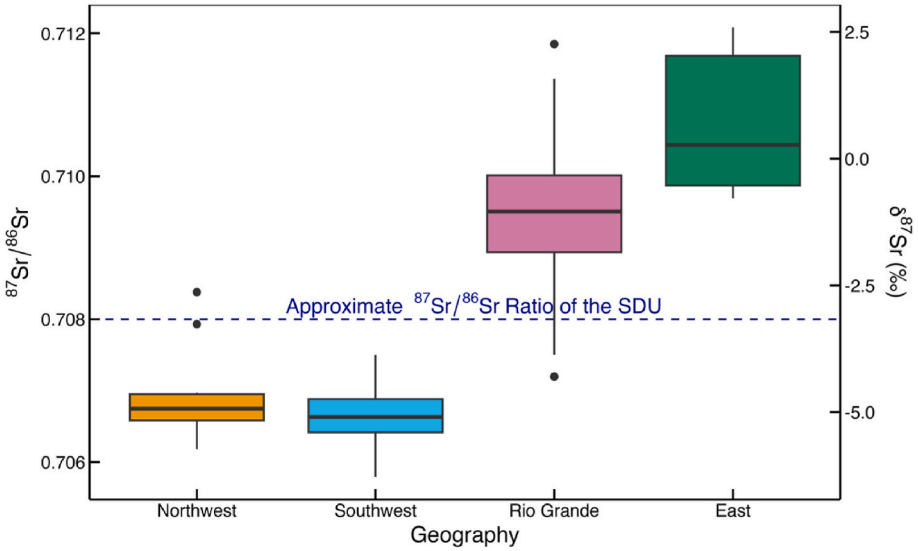

Fig. 7. Boxplot of $^{87}Sr/^{86}Sr$ isotopic compositions in water samples across the SDU regions; from left to right; northwest (orange), southwest (blue), Rio Grande (pink), and east (green). The dark blue dashed line represents the approximate $^{87}Sr/^{86}Sr$ ratio of the SDU (Williams et al., 2025b). The two outliers northwestern samples are the northernmost samples in the region, near the SDU. (For interpretation of the references to color in this figure legend, the reader is referred to the Web version of this article.)

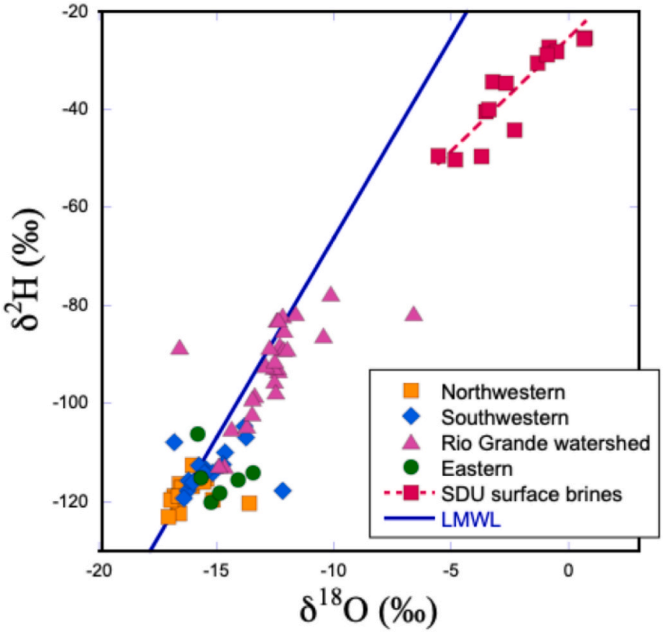

Fig. 8. *Variations of $\delta^{18}O$ and δ^2H in groundwater sorted by the geographical regions in comparison to the composition of surface brines from the Salar de Uyuni (Williams et al., 2026) and Local Meteoric Water Line (LMWL; Chaffaut et al. (1998)). Note that most of the groundwater samples had $\delta^{18}O$ and δ^2H values with a slope associated to the LMWL with a slope of 8 relative to the SDU brines with higher values and a δ^2H- $\delta^{18}O$ slope <8.*

dependent leaching experiments reported in Yuan et al. (2021).

In contrast, the high B/Li ratios in the shallow groundwater in the northwest (median = 20) and southwest (70) are not consistent the ratios detected in volcanic rocks of the central Andes. Previous studies have detected Li concentrations in volcanic rocks of the Central Andes varying between median values of 16.1 ppm (n = 706; Mamani et al. (2010)) to 20 ppm (n = 53; Meixner et al. (2020)) whereas B (a less commonly measured element in rocks) concentrations have a median value of ~20 ppm reported by Rosner et al. (2003) (n = 20) and Shinjoe et al. (2013) (n = 30). Muller et al. (2020) reported higher concentration values of Li (median of 147 ppm) and B (60 ppm) in volcanic rocks of Pastos Grande located upstream to the Rio Grande watershed in Bolivia. Consequently, the B/Li ratios in volcanic rocks vary from <1 to ~1, which are lower than the ratios detected in the shallow groundwater. Previous reported data (Risacher et al., 2003; Risacher and Fritz, 2009) and data compiled by Williams and Vengosh (2026) show relative higher B/Li ratios in low salinity groundwater from the Central Andes with a median value of 9.5 (for groundwater with TDS<1000 mg/L; n = 261). The observation of a higher B/Li in low-saline groundwater is consistent with the results of multiple experimental studies that have shown that low-temperature weathering process commonly generates preferential B mobilization relative to Li, mostly due to the partial incorporation of Li into smectite, zeolite, or other secondary aluminosilicates phases, while B remains more mobile into the aquatic solution (Millot et al., 2010; Pistiner and Henderson, 2003). One would argue, however, that the arid conditions in the high Altiplano region would not promote intensive weathering secondary minerals (Godfrey et al., 2013, 2019) and that the high B/Li reflects preferential leaching of B over Li from the volcanic rocks, related to the occurrence of B in the more soluble phases (e.g., glass) of the volcanic rocks (Shaw and Sturchio, 1992).

It should be noted that the water-rock interactions with the andesitic rocks from the western cordillera have resulted in conspicuously high B concentrations despite the relatively low salinity of the groundwater relative to the other regions. Therefore, the occurrence of B above the WHO recommended drinking water level is directly linked to these volcanic rocks. The inverse correlation between B/Li and $^{87}Sr/^{86}Sr$ ratios in groundwater from the northwest and southwest regions (Fig. S8) further reinforce our hypothesis that the high boron content is derived from greater water-rock interactions with volcanic rocks of the western cordillera in which the distinctive low $^{87}Sr/^{86}Sr$ fingerprint of the local lithology is becoming more prominent with greater B/Li ratios, and therefore, having a greater impact on the composition of the local groundwater.

The stable isotope variations show different recharge patterns in the shallow groundwater surrounding the SDU. While the low salinity groundwater from the northwestern and southwestern areas have relatively low $\delta^{18}O$ and δ^2H associated with the GMWL (Fig. 8), low salinity groundwater from Rio Grande watershed has much higher $\delta^{18}O$ and δ^2H

along the GMWL. This difference suggests that the recharge waters in the western areas are derived from higher elevation sources (Gonfiantini et al., 2001) associated with the western Cordilleras, whereas recharge in the Rio Grande watershed is more local from a lower elevation source. It is important to note that the relatively higher $\delta^{18}O$ and $\delta^{2}H$ values in the low salinity groundwater from the Rio Grande watershed do not deviate from the LMWL, inferring that the higher values are not the result of evaporative processes.

4.2. Tracing the sources of the saline groundwater

Saline groundwater (i.e., TDS> 1000 mg/L) was detected across the different areas surrounding the SDU (Fig. 3). We hypothesize that the saline groundwater can be derived from the following sources: (1) in-situ evaporation of the shallow groundwater/spring; (2) mixing with the nearby subsurface SDU brines; and (3) mixing with underlying geothermal waters. Each of these sources has a unique and distinct geochemical fingerprint that can be used to delineate the source(s) of the saline groundwater. The SDU brine has distinctly high $\delta^{18}O$ and $\delta^{2}H$ values with a lower $\delta^{18}O$-$\delta^{2}H$ slope than the LMWL (Fig. 8) as well as a narrow range of $^{87}Sr/^{86}Sr$ ratios of ~0.7086 (Williams et al., 2026). We expect that in-situ evaporation would result in a similar deviation of the $\delta^{18}O$-$\delta^{2}H$ slope from the LMWL. To evaluate the geochemical fingerprint of a possible geothermal source, we have evaluated the geochemistry of geothermal waters located across the Bolivian Altiplano north of SDU reported by Morteani et al. (2014) and Ormachea Muñoz et al. (2015) as well as geothermal waters from Laguna Pastos Grandes south of SDU reported by Muller et al. (2020) (Table S2). The data of the geothermal water show a wide range of salinity, ranging from low salinity (Cl = 50 mg/L) to highly saline water (Cl = 10,000 mg/L) with Na/Cl~0.95, low Ca/Cl and Mg/Cl ratios, conspicuously low SO_4/Cl ratios, as well as low Mg/Li ratios (median for all geothermal water = 3, 1 for the highest salinity water) and B/Li (median = 1.2; n = 25) ratios (Fig. 6). Relationship between Mg and Li are commonly employed as a geothermometer where Mg is preferentially removed from the system at higher temperatures due to retention by secondary minerals (Kharaka and Mariner, 1989; Li et al., 2021). In contrast, Li is effectively mobilized from the rock and remains relatively soluble resulting in low Mg/Li ratios in geothermal fluids (Kharaka and Mariner, 1989). The viability of the Mg/Li ratio has been demonstrated as an effective proxy of the relative temperature of solute origins for spring waters across the altiplano where low temperature water-rock interactions are shown to produce high Mg/Li ratios whereas high temperature water-rock interactions result in low Mg/Li ratios (Williams and Vengosh, 2026).

The inverse relationships between Mg/Li and B/Li with salinity (Fig. 6) and the positive association between B/Li and Mg/Li ratios (Fig. 9) are consistent with the B/Li and Mg/Li variations of the geothermal water across the Bolivian Altiplano. To further evaluate this association, we conducted mixing modeling between the highest salinity geothermal water of the Laguna Pastos Grandes located south of SDU (data from Muller et al., 2020) and two endmembers of low-saline groundwater from this study. In the mixing model we mix the B, Mg, and Li concentrations as referenced to Cl, assuming it is a conservative component. Nonetheless, the mixing modeling conducted for the saline geothermal water and two types of low-saline groundwater show consistent trends with the variations of the B/Li and Mg/Li ratios (Figs. 6 and 9), suggesting that the geothermal water is the source for the saline shallow groundwater. Based on the mixing model we estimate that shallow groundwater with Cl > 1000 mg/L correspond to ~20% contribution of the saline geothermal water (Fig. 6). However, the large geochemical variations of the geothermal waters could infer a different geothermal water endmember with lower salinity, which would infer in a larger fractional contribution of the geothermal water in the saline shallow groundwater.

Another important parameter that rules out the effects of salinization from mixing with SDU brine is the systematic $\delta^{18}O$-$\delta^{2}H$ slope of ~8 of most of the shallow groundwater samples relative to the much higher $\delta^{2}H$ and $\delta^{18}O$ values with a $\delta^{18}O$-$\delta^{2}H$ slope <8 that characterizes the SDU brines (Fig. 8). Since the O and H isotopes would reflect the direct water molecule mixing relationships, any small contribution of the SDU brine in a possible blend would shift the $\delta^{18}O$-$\delta^{2}H$ slope towards higher values and a <8 slope. This phenomenon was not observed, indicating

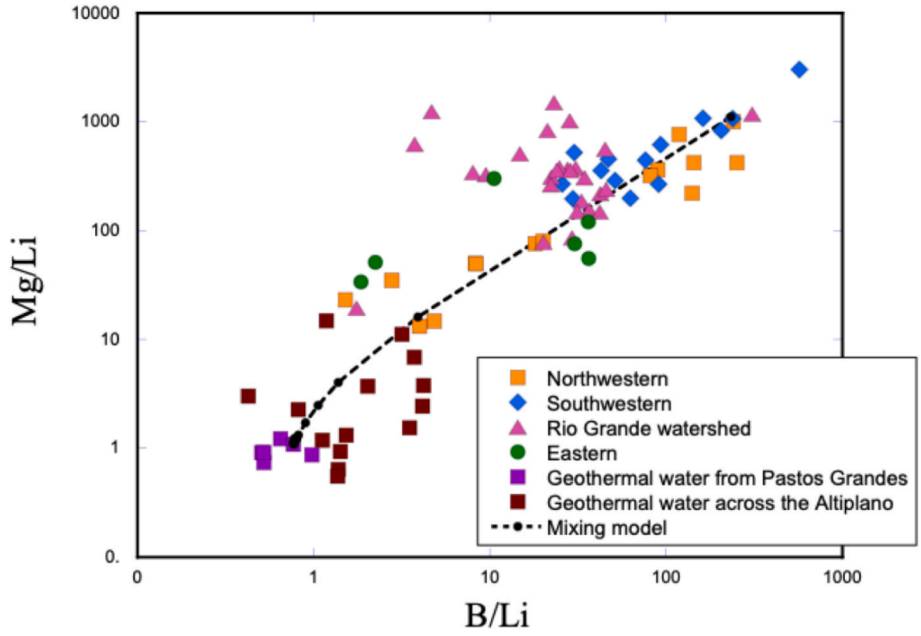

Fig. 9. Mg/Li ratios versus B/Li ratios in all low salinity (TDS<1000) groundwaters from this study (blue circles), saline groundwaters (TDS>1000) from this study (yellow squares), surface waters from this study (green diamonds), brines from Williams et al. (2025b), and thermal water data from Muller et al. (2020) and Morteani et al. (2014). The correlation of Mg/Li and B/Li ratios is associated with the variations of the mixing modeling conducted in this study between saline geothermal water with low Mg/Li and B/Li ratios and low-saline groundwater with high Mg/Li and B/Li ratios (dashed line). (For interpretation of the references to color in this figure legend, the reader is referred to the Web version of this article.)

no impact of the SDU brines. In contrast, it has been shown that $\delta^{18}O$ and $\delta^{2}H$ in the geothermal water in the Bolivian Altiplano falls along the LMWL with a slope of ~8 with relatively low $\delta^{18}O$ and $\delta^{2}H$ values (Morteani et al., 2014). Therefore, mixing of the shallow groundwater with local geothermal water would not affect the $\delta^{18}O$ and $\delta^{2}H$ variations nor their meteoric water characterization (i.e., a $\delta^{18}O$-$\delta^{2}H$ slope ~8).

We have identified several saline groundwater sites with low B/Li ratios (a range of 0.97-12.9) that could indicate the occurrence of geothermal waters rather than other saline sources, such as SDU brines (Fig. 9). In the northwest region, these include 4 sites near Tahua on the margin of the SDU, with low B/Li and high TDS (Fig. S6). However, one would suggest that high saline groundwater along the border of the SDU brine, which contains high TDS and low B/Li, could be attributed to mixing with subsurface hypersaline SDU brines rather than geothermal water. However, the low $^{87}Sr/^{86}Sr$ ratios detected in the saline groundwater (~0.706; $\delta^{87}Sr$ = -5.97‰) are different from the relatively high $^{87}Sr/^{86}Sr$ of the SDU brine (0.7087; $\delta^{87}Sr$ = -2.17‰; Williams et al., 2026), which does not support mixing with the SDU brine. Rather, we suggest that the low B/Li and Mg/Li of the saline groundwater reflect mixing with underlying geothermal waters, and that the less radiogenic Sr isotope ratios reflect water-rock interactions with local lithology of the western cordillera. Similarly, a saline spring west of the Rio Grande watershed with high TDS and low B/Li also mimics the Sr isotope ratio of the western cordillera isotope composition, suggesting the presence of geothermal water. Likewise, we have also detected multiple sites elsewhere in the study area that suggest similar geothermal origins (Fig. 10). Two saline springs in the east with high TDS also have low B/Li and low Mg/Li ratios (Fig. 10). The $^{87}Sr/^{86}Sr$ ratios there are more radiogenic (~0.711; $\delta^{87}Sr$ = 1.06‰), and therefore also reflect water-rock interaction with the local lithology of the eastern cordillera with high $^{87}Sr/^{86}Sr$ rather than mixing with subsurface SDU brines. Overall, given that the Sr isotopes ratios of the saline groundwater from the western and eastern areas are consistent with the compositions of waters draining the respective cordilleras rocks and not SDU brines, the Sr isotope data reinforces our hypothesis for the geothermal source of the saline groundwater in the vicinity of the SDU.

4.3. Geochemical behavior of arsenic

Our data indicate that As levels above the WHO drinking water recommendation occur in both low- and high salinity groundwater (Fig. 11). Therefore, we link the As occurrence for both mobilization of As from the local lithology through low temperature water-rock interactions as well as mixing with the As-rich geothermal water. It should be noted that the occurrence of As above 10 µg/L is distributed across all regions, indicating that water-rock interactions with the lithology of both the eastern and western cordillera results in similar As mobilization into the groundwater. Across all regions, the maximum As concentrations are associated with low B/Li ratios, indicating a geothermal source (Fig. S7). In contrast, some saline groundwater had up to an order of

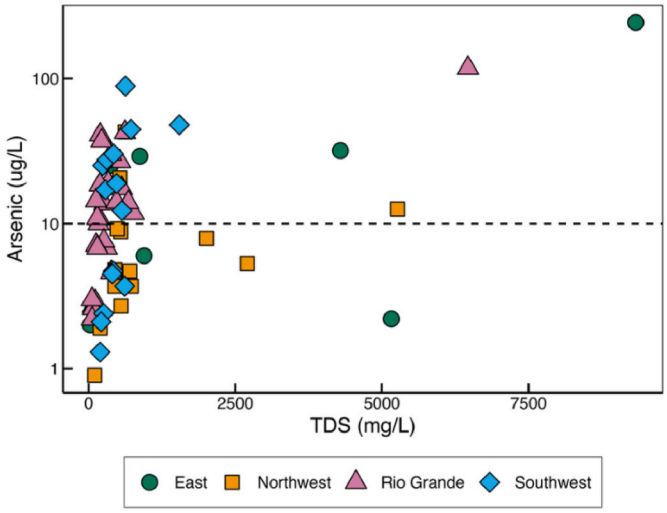

Fig. 11. *Arsenic (µg/L) versus TDS (mg/L) in groundwater samples from the northwest (orange squares), east (green circles), southwest (blue diamonds), and Rio Grande (pink triangles).* (For interpretation of the references to color in this figure legend, the reader is referred to the Web version of this article.)

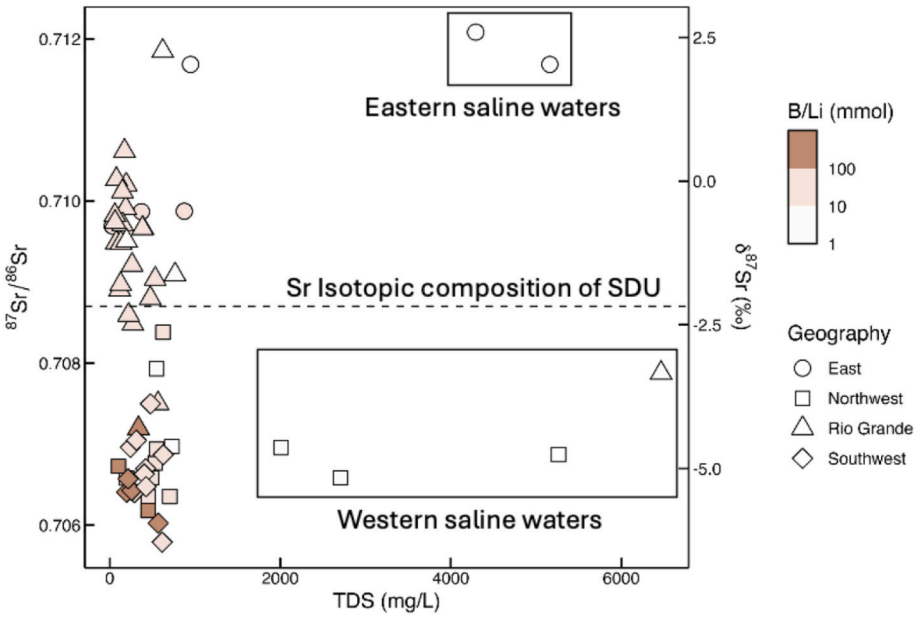

Fig. 10. $^{87}Sr/^{86}Sr$ and $\delta^{87}Sr$ (‰) versus TDS (mg/L) in groundwater from the east (circles), northwest (squares), southwest (diamonds), and Rio Grande (triangle) regions. Waters are colored by the variations of the B/Li molar ratios, with B/Li < 10 as white, B/Li from 10 to 100 in beige, and B/Li > 100 in dark brown. The Sr isotopic composition of the SDU brine is denoted by a dashed black line. (For interpretation of the references to color in this figure legend, the reader is referred to the Web version of this article.)

magnitude higher As content, reflecting the larger contribution of As from the geothermal source commonly enriched in As.

The modeled speciation of As reveals the vast majority (>99%) of As occurrence in the shallow groundwater is in the form of the oxidized arsenate species (As(V); see Fig. S11) in nearly all samples collected. This is consistent with low concentrations of other redox-sensitive elements such as Mn and Fe in the shallow groundwater. Our modeling results are consistent with As speciation data reported in previous studies; Tapia et al. (2019) have reported that 90% of As found in surface and groundwaters across the Altiplano occurs in the As(V) species. Other studies have shown that geothermal springs also contain As (III), however it has been suggested to quickly oxidize to the As(V) upon exposure to oxidizing conditions near the surface (Ormachea Muñoz et al., 2015; Tapia et al., 2019).

4.4. Community health and broader implications

Our data indicates that communities in the SDU watershed are currently exposed to one or more contaminants above the WHO drinking water recommendation limits through consumption of the local shallow groundwater. Future large scale lithium extraction from the SDU will require extensive water use in this arid zone and therefore massive groundwater pumping is expected. Large-scale groundwater extraction will likely result in drawdown of groundwater levels and potentially desiccation and/or further contamination of the already impaired water resources. Such impacts have been shown in the Salar de Atacama (SDA) in Chile, where large-scale lithium brine pumping for Li exploration over the last three decades has resulted in drawdown of the water table within the salt pan, which has triggered localized surface subsidence (Flexer et al., 2018; Marazuela et al., 2019, 2020; Bustos-Gallardo et al., 2021; Vera et al., 2023). Likewise, we hypothesize that climate change, which could alter precipitation patterns in the Altiplano region, could reduce groundwater replenishment and thus groundwater levels. As demonstrated in this study, saline groundwater detected in the vicinity of the SDU watershed is originated from mixing with underlying geothermal waters. Therefore, projected large-scale groundwater pumping for lithium extraction and/or climate change effects will likely induce further salinization and increase the occurrences of trace elements hazardous to human health in the shallow groundwater resources currently used by the local communities. In some other areas in the Central Andes previous studies have shown that groundwater chemistry is influenced by mixing with geothermal waters and that shallow groundwaters often have a geothermal component (Rissmann et al., 2015; Williams and Vengosh, 2026). Consequently, extensive water pumping resulted from large-scale Li extraction could likely reduce water availability as well as degrade the quality of the already impaired local groundwater resources.

We have mapped out the communities that are at the highest risks of geothermal water contamination to occur in the low-lying areas in proximity to the SDU, where groundwater sites are already saline as illustrated in Fig. 12. The projected salinization will likely increase the concentrations of B, Li, and As in the groundwater resources. However, groundwater from the western cordillera is currently characterized by conspicuously high B independent of salinity, which also poses human health risks to the local populations.

Exposure to these elements through consumption of contaminated drinking water has been shown to produce a wide spectrum of health effects in humans. Chronic exposure to As in drinking water at concentrations of 10 μg/L or greater poses serious long term health risks, such as skin lesions and cancer of the lung, kidney, and bladder (WHO, 2003). In Latin America, exposure to heightened levels of As (>50 μg/L) has been estimated to impact up to 4.5 million people (McClintock et al., 2012). However, recent work has suggested that continuous and long term exposure to geogenic As over generations in indigenous Andean communities, particularly in Bolivia, has prompted genetic selection to allow for higher As tolerance within individuals (Eichstaedt et al., 2015; de Loma et al., 2022).

Studies indicate that excessive B consumption is linked to developmental and reproductive issues in males, such as low sperm count, impaired fetal growth, and fetal skeletal malformations (Weir and Fisher, 1972; Price et al., 1996). In northern Argentina in Andean communities near San Antonio de los Cobres, where B concentrations in drinking water reach up to 5956 μg/L far exceeding the WHO recommendation of 2400 μg/L, it has been demonstrated that there is an inverse correlation between B concentration in maternal serum and newborn birth weight, birth length, and head circumference (Harari et al., 2012; Igra et al., 2016). The long-term health implications of this phenomenon are currently not well understood but stand to impact large populations in the Altiplano that are regularly exposed to elevated B in drinking water.

Exposure to elevated Li in drinking water has also shown to induce a wide range of toxicological effects. Lithium is used as a drug to treat bipolar disorder; however, a listed potential side-effect of Li medication is reduced thyroid function. Negatively impacted thyroid function has been observed in Andean women connected to chronic consumption of drinking water with high Li concentrations (Broberg et al., 2011). Likewise, in pregnant Andean women impaired thyroid function induced by Li exposure may negatively impact fetal development (Harari et al., 2015). In contrast, recent genotoxicity work has suggested that elevated Li content in drinking waters in Bolivia may exhibit a protective effect against DNA strand breaks inflicted by co-occurring As exposure (Tirado et al., 2024).

It should be noted that Andean indigenous populations have been routinely exposed to As, B, and Li contaminants regularly for thousands of years, as evidenced by elevated As, B and Li detected within well preserved mummy hairs (Blumenstiel et al., 2020; Arriaza et al., 2021; Amarasiriwardena et al., 2023). Nonetheless, the long-term and/or confounding human health implications of co-exposures to Li, B, and/or As, especially in populations with some evolved genetic resistance, remains poorly understood and warrants further investigation.

5. Conclusion

This study presents, for a first time, a comprehensive groundwater quality investigation in shallow groundwater resources used by indigenous local communities surrounding the SDU in Bolivia. The data show elevated levels of salinity, As, B, and Li levels in the shallow groundwater, where As and B concentrations exceeded the WHO recommended limits for drinking water in 50.2% and 42.9% of the investigated waters, respectively. Although there is no WHO threshold value for Li, observed concentrations span four orders of magnitude and increase linearly with salinity. This study presents key geochemical indicators including elemental ratios of B/Li, Mg/Li, stable isotopes of $\delta^{18}O$ and $\delta^{2}H$, and Sr isotopes ($^{87}Sr/^{86}Sr$) for delineating the source of the groundwater. The results show a distinction between groundwater effected by low-temperature water-rock interactions with local volcanic lithology and groundwater likely salinized by mixing with geothermal waters. We demonstrate that low-temperature water-rock interaction with the local lithology generates low salinity groundwater with $\delta^{18}O$ and $\delta^{2}H$ composition that mimics the LMWL, as well as high B/Li and Mg/Li ratios, as opposed to the saline groundwater with low B/Li and Mg/Li ratios that also characterize the composition of geothermal waters. The integration of the geochemical proxies developed in this study can provide useful insights to detect the impact of underlying geothermal water on shallow groundwater in the vicinity of the SDU that can be applied elsewhere in the Altiplano. We conducted a mixing model to predict possible mixing between the low-salinity and saline geothermal water to demonstrate and quantify groundwater salinization by underlying geothermal influenced water. Based on evidence from Salar de Atacama in Chile, we predict that future large-scale groundwater pumping for enhanced lithium extraction in the SDU as well as possible changes in precipitation patterns induced by climate change could cause

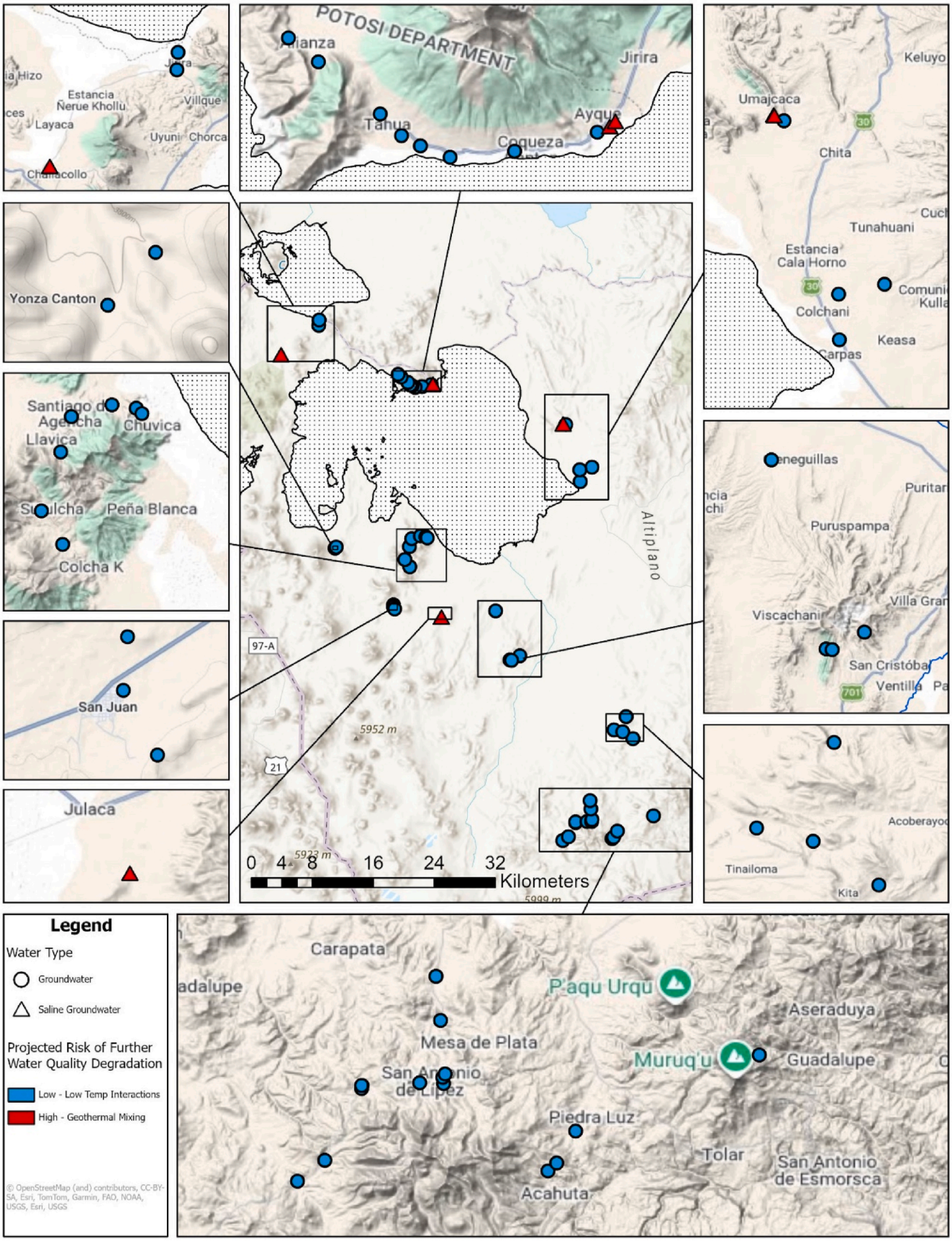

Fig. 12. Map depicting the locations of projected water quality degradation risks in groundwater (circles) in communities surrounding the SDU). Low risks are represented by blue circles, and high risks by red circles. (For interpretation of the references to color in this figure legend, the reader is referred to the Web version of this article.)

drawdown of groundwater level and even desiccation of shallow wells and springs used as the sole water resource for the local communities. Using the geochemical indicators for geothermal water contribution, this study highlights sensitive areas in which drawdown of groundwater level might further increase the impact of the underlying geothermal waters and further degradation of the water quality, which could affect the communities that presently, almost solely on the local shallow groundwater.

CRediT authorship contribution statement

Hannah Wudke: Writing – original draft, Visualization, Investigation, Formal analysis. **Gordon D.Z. Williams:** Writing – review & editing, Writing – original draft, Visualization, Software, Methodology, Investigation, Formal analysis. **Avner Vengosh:** Writing – review & editing, Writing – original draft, Validation, Supervision, Resources, Project administration, Methodology, Investigation, Funding acquisition, Conceptualization.

Declaration of competing interest

The authors declare that they have no known competing financial interests or personal relationships that could have appeared to influence the work reported in this paper.

Acknowledgements

This work was funded by the Duke University Climate Research Innovation Seed Program (CRISP) and the Duke University Josiah Charles Trent Memorial Foundation Endowment Fund. The authors would like to specially thank Y. Cruz and the Federación Regional Única de Trabajadores Campesinos del Altiplano Sur (FRUTCAS) for facilitating sample permissioning, coordination, and collection. We thank K. Ledebur from the Andean Information Network and R. Calizaya for assisting with our sampling campaign, and for providing guidance with field navigation and coordination with communities. We thank the editor and three anonymous reviewers for their thorough and detailed reviews, which have improved the quality of this paper.

Appendix A. Supplementary data

Supplementary data to this article can be found online at https://doi.org/10.1016/j.apgeochem.2026.107053.

Data availability

All data are provided in the paper.

References

Álvarez-Amado, F., Tardani, D., Poblete-González, C., Godfrey, L., Matte-Estrada, D., 2022. Hydrogeochemical processes controlling the water composition in a hyperarid environment: new insights from Li, B, and Sr isotopes in the Salar de Atacama. Sci. Total Environ. 835, 155470. https://doi.org/10.1016/j.scitotenv.2022.155470.

Amarasiriwardena, D., Ahmed, M., Arriaza, B., 2023. Environmental arsenic exposure by ancient andeans: measurement of As in mummy hair using LA-ICP-MS. J. Archaeolog. Sci.: Rep. 48, 103883. https://doi.org/10.1016/j.jasrep.2023.103883.

Araoka, D., Kawahata, H., Takagi, T., Watanabe, Y., Nishimura, K., Nishio, Y., 2014. Lithium and strontium isotopic systematics in playas in Nevada, USA: constraints on the origin of lithium. Miner. Deposita 49, 371–379. https://doi.org/10.1007/s00126-013-0495-y.

Arriaza, B., Blumenstiel, D., Amarasiriwardena, D., Standen, V.G., Vizcarra, A., 2021. Five thousand years of bellyaches: exploring boron concentration in ancient populations of the atacama desert. Am. J. Phys. Anthropol. 174, 254–267. https://doi.org/10.1002/ajpa.24155.

Baker, P.A., Rigsby, C.A., Seltzer, G.O., Fritz, S.C., Lowenstein, T.K., Bacher, N.P., Veliz, C., 2001. Tropical climate changes at millennial and orbital timescales on the Bolivian altiplano. Nature 409, 698–701. https://doi.org/10.1038/35055524.

Banks, D., Markland, H., Smith, P.V., Mendez, C., Rodriguez, J., Huerta, A., Sæther, O.M., 2004. Distribution, salinity and pH dependence of elements in surface waters of the catchment areas of the salars of coipasa and uyuni, Bolivian altiplano. J. Geochem. Explor. 84, 141–166. https://doi.org/10.1016/j.gexplo.2004.07.001.

Blumenstiel, D., McDonald, M., Arriaza, B., Amarasiriwardena, D., 2020. Exposure to geogenic lithium in ancient Andeans: unraveling lithium in mummy hair using LA-ICP-MS. J. Archaeol. Sci. 113, 105062. https://doi.org/10.1016/j.jas.2019.105062.

Broberg, K., Concha, G., Engström, K., Lindvall, M., Grandér, M., Vahter, M., 2011. Lithium in drinking water and thyroid function. Environ. Health Perspect. 119, 827–830. https://doi.org/10.1289/ehp.1002678.

Bustos-Gallardo, B., Bridge, G., Prieto, M., 2021. Harvesting Lithium: water, brine and the industrial dynamics of production in the Salar de Atacama. Geoforum 119, 177–189. https://doi.org/10.1016/j.geoforum.2021.01.001.

Chaffaut, I., Coudrain-Ribstein, A., Michelot, J.-L., Pouyaurd, B., 1998. Précipitations d'altitude du nord-Chili, origine des sources de vapeur et données isotopiques. Bull. Inst. Fr. Détudes Andin. 27, 367–384.

Concha, G., Broberg, K., Grandér, M., Cardozo, A., Palm, B., Vahter, M., 2010. High-level exposure to lithium, boron, cesium, and arsenic via drinking water in the andes of northern Argentina. Environ. Sci. Technol. 44, 6875–6880. https://doi.org/10.1021/es1010384.

Cortes-Calderon, E.A., Ellis, B.S., Tavazzani, L., Magna, T., Harris, C., Benson, T.R., 2025. Lithium Inventory of the Cerro Galán Volcanic System (Argentina): the Role of Magmatism as a Source for Li-Bearing Brine Deposits.

de Loma, J., Vicente, M., Tirado, N., Ascui, F., Vahter, M., Gardon, J., Schlebusch, C.M., Broberg, K., 2022. Human adaptation to arsenic in bolivians living in the andes. Chemosphere 301, 134764. https://doi.org/10.1016/j.chemosphere.2022.134764.

de Silva, S., Zandt, G., Trumbull, R., Viramonte, J.G., Salas, G., Jiménez, N., 2006. Large ignimbrite eruptions and volcano-tectonic depressions in the central andes: a thermomechanical perspective. In: Troise, C., Natale, G.D., Kilburn, C.R.J. (Eds.), Mechanisms of Activity and Unrest at Large Calderas. Geological Society of London. https://doi.org/10.1144/GSL.SP.2006.269.01.04.

Del Bono, D.A., Borda, L.G., Godfrey, L.V., Chiaramonte, N.L., Balbis, C., Pasquini, A.I., García, M.G., 2026. Mineralogical and chemical transformations of volcanic ash and rocks through interaction with water: insights into the genesis of lithium deposits in puna brines. Miner. Deposita. https://doi.org/10.1007/s00126-026-01428-5.

Eichstaedt, C.A., Antao, T., Cardona, A., Pagani, L., Kivisild, T., Mormina, M., 2015. Positive selection of AS3MT to arsenic water in Andean populations. Mutat. Res. Fundam. Mol. Mech. Mutagen. 780, 97–102. https://doi.org/10.1016/j.mrfmmm.2015.07.007.

Ellis, B.S., Szymanowski, D., Harris, C., Tollan, P.M.E., Neukampf, J., Guillong, M., Cortes-Calderon, E.A., Bachmann, O., 2022. Evaluating the potential of rhyolitic glass as a lithium source for brine deposits. Econ. Geol. 117, 91–105. https://doi.org/10.5382/econgeo.4866.

Eugster, H.P., Hardie, L.A., 1978. Saline Lakes. In: Lerman, A. (Ed.), Lakes: Chemistry, Geology, Physics. Springer, New York, NY, pp. 237–293. https://doi.org/10.1007/978-1-4757-1152-3_8.

Flexer, V., Baspineiro, C.F., Galli, C.I., 2018. Lithium recovery from brines: a vital raw material for green energies with a potential environmental impact in its mining and processing. Sci. Total Environ. 639, 1188–1204. https://doi.org/10.1016/j.scitotenv.2018.05.223.

Fornari, M., Risacher, F., Féraud, G., 2001. Dating of paleolakes in the central altiplano of Bolivia. Palaeogeogr. Palaeoclimatol. Palaeoecol. 172, 269–282. https://doi.org/10.1016/S0031-0182(01)00301-7.

Godfrey, L.V., Chan, L.-H., Alonso, R.N., Lowenstein, T.K., McDonough, W.F., Houston, J., Li, J., Bobst, A., Jordan, T.E., 2013. The role of climate in the accumulation of lithium-rich brine in the central andes. Appl. Geochem. 38, 92–102. https://doi.org/10.1016/j.apgeochem.2013.09.002.

Godfrey, L.V., Herrera, C., Gamboa, C., Mathur, R., 2019. Chemical and isotopic evolution of groundwater through the active Andean arc of northern Chile. Chem. Geol. 518, 32–44. https://doi.org/10.1016/j.chemgeo.2019.04.011.

Gonfiantini, R., Roche, M.-A., Olivry, J.-C., Fontes, J.-C., Zuppi, G.M., 2001. The altitude effect on the isotopic composition of tropical rains. Chem. Geol. 181, 147–167. https://doi.org/10.1016/S0009-2541(01)00279-0.

Grove, M.J., Baker, P.A., Cross, S.L., Rigsby, C.A., Seltzer, G.O., 2003. Application of strontium isotopes to understanding the hydrology and paleohydrology of the altiplano, Bolivia–Peru. Palaeogeogr. Palaeoclimatol. Palaeoecol. 194, 281–297. https://doi.org/10.1016/S0031-0182(03)00282-7.

Hall, G.A., Williams, G.D.Z., Sirbescu, M.-L.C., Lu, P.L., Dwyer, G.S., Richter, D.D., Vengosh, A., 2025. Strontium isotopes and Rb/Sr tracers in surface soils for locating subsurface lithium pegmatites. Appl. Geochem. 195, 106631. https://doi.org/10.1016/j.apgeochem.2025.106631.

Harari, F., Bottai, M., Casimiro, E., Palm, B., Vahter, M., 2015. Exposure to lithium and cesium through drinking water and thyroid function during pregnancy: a prospective cohort study. Thyroid 25, 1199–1208. https://doi.org/10.1089/thy.2015.0280.

Harari, F., Ronco, A.M., Concha, G., Llanos, M., Grandér, M., Castro, F., Palm, B., Nermell, B., Vahter, M., 2012. Early-life exposure to lithium and boron from drinking water. Reprod. Toxicol. 34, 552–560. https://doi.org/10.1016/j.reprotox.2012.08.009.

Hill, R.C., Pieńkowska, A., Merbach, I., Reitz, T., Muehe, E.M., Vengosh, A., 2025. Impacts of fertilization on metal(loid) transfer from soil to wheat in a long-term fertilization experiment – using 87Sr/86Sr isotopes as metal(loid) tracer. Environ. Int. 205, 109851. https://doi.org/10.1016/j.envint.2025.109851.

Hofstra, A.H., Todorov, T.I., Mercer, C.N., Adams, D.T., Marsh, E.E., 2013. Silicate melt inclusion evidence for extreme pre-eruptive enrichment and post-eruptive depletion of lithium in silicic volcanic rocks of the Western United States: implications for the origin of lithium-rich brines. Econ. Geol. 108, 1691–1701. https://doi.org/10.2113/econgeo.108.7.1691.

Horton, R., 1965. An Index Number System for Rating Water Quality, vol. 37, pp. 292–315.
Igra, A.M., Harari, F., Lu, Y., Casimiro, E., Vahter, M., 2016. Boron exposure through drinking water during pregnancy and birth size. Environ. Int. 95, 54–60. https://doi.org/10.1016/j.envint.2016.07.017.
International Energy Agency, 2021. The Role of Critical Minerals in Clean Energy Transitions. OECD. https://doi.org/10.1787/f262b91c-en.
Jaskula, B.W., 2024. Lithium, Mineral Commodities Summary 2024 U.S. Geological Survey.
Jochum, K.P., Nohl, U., Herwig, K., Lammel, E., Stoll, B., Hofmann, A.W., 2005. GeoReM: a new geochemical database for reference materials and isotopic standards. Geostand. Geoanal. Res. 29, 333–338. https://doi.org/10.1111/j.1751-908X.2005.tb00904.x.
Kasemann, S.A., Meixner, A., Erzinger, J., Viramonte, J.G., Alonso, R.N., Franz, G., 2004. Boron isotope composition of geothermal fluids and borate minerals from Salar deposits (central Andes/NW Argentina). J. South Am. Earth Sci. 16, 685–697. https://doi.org/10.1016/j.jsames.2003.12.004.
Kesler, S.E., Gruber, P.W., Medina, P.A., Keoleian, G.A., Everson, M.P., Wallington, T.J., 2012. Global lithium resources: relative importance of pegmatite, brine and other deposits. Ore Geol. Rev. 48, 55–69. https://doi.org/10.1016/j.oregeorev.2012.05.006.
Kharaka, Y.K., Mariner, R.H., 1989. Chemical geothermometers and their application to formation waters from sedimentary basins. In: Naeser, N.D., McCulloh, T.H. (Eds.), Thermal History of Sedimentary Basins. Springer, New York, New York, NY, pp. 99–117. https://doi.org/10.1007/978-1-4612-3492-0_6.
Kirshen, A.B., Moran, B.J., Munk, L.A., Russo, A.A., McKnight, S.V., Jenckes, J., Corkran, D.B., Bresee, M., Boutt, D.F., 2025. Freshwater inflows to closed basins of the andean Plateau in Chile, Argentina, and Bolivia. Commun. Earth Environ. 6, 177. https://doi.org/10.1038/s43247-025-02130-6.
Krabbenhöft, A., Fietzke, J., Eisenhauer, A., Liebetrau, V., Böhm, F., Vollstaedt, H., 2009. Determination of radiogenic and stable strontium isotope ratios (87Sr/86Sr; δ88/86Sr) by thermal ionization mass spectrometry applying an 87Sr/84Sr double spike. J. Anal. At. Spectrom. 24, 1267–1271. https://doi.org/10.1039/b906292k.
Li, J., Sagoe, G., Wang, X., Yang, Z., 2021. Assessing the suitability of lithium-related geothermometers for estimating the temperature of felsic rock reservoirs. Geothermics 89, 101950. https://doi.org/10.1016/j.geothermics.2020.101950.
Lima, I.Q., Muñoz, M.O., Ramos, O.E.R., Bhattacharya, P., Choque, R.Q., Aguirre, J.Q., Sracek, O., 2019. Hydrochemical assessment with respect to arsenic and other trace elements in the lower katari basin, Bolivian altiplano. Groundw. Sustain. Dev. 8, 281–293. https://doi.org/10.1016/j.gsd.2018.11.013.
Liu, W., Agusdinata, D.B., 2020. Interdependencies of lithium mining and communities sustainability in Salar de Atacama, Chile. J. Clean. Prod. 260, 120838. https://doi.org/10.1016/j.jclepro.2020.120838.
Mamani, M., Wörner, G., Sempere, T., 2010. Geochemical variations in igneous rocks of the Central andean orocline (13°S to 18°S): tracing crustal thickening and magma generation through time and space. GSA Bull 122 (1), 162–182. https://doi.org/10.1130/B26538.
Marazuela, M.A., Vázquez-Suñé, E., Ayora, C., García-Gil, A., 2020. Towards more sustainable brine extraction in salt flats: learning from the Salar de Atacama. Sci. Total Environ. 703, 135605. https://doi.org/10.1016/j.scitotenv.2019.135605.
Marazuela, M.A., Vázquez-Suñé, E., Ayora, C., García-Gil, A., Palma, T., 2019. The effect of brine pumping on the natural hydrodynamics of the Salar de Atacama: the damping capacity of salt flats. Sci. Total Environ. 654, 1118–1131. https://doi.org/10.1016/j.scitotenv.2018.11.196.
McArthur, J.M., Millar, I.L., Drury, A.J., Wagner, D., 2025. Strontium-isotope stratigraphy: methodology, standard values (SRM987, EN-1, E&A), a new Neogene curve of 87Sr/86Sr against time, its implications for astrochronology ([I]ODP sites 1146, 1264, U1337, and U1338), and its application to ODP site 758 (Indian summer monsoon) and IODP site 1120 (A new age-model). Palaeogeogr. Palaeoclimatol. Palaeoecol. 669, 112907. https://doi.org/10.1016/j.palaeo.2025.112907.
McClintock, T.R., Chen, Y., Bundschuh, J., Oliver, J.T., Navoni, J., Olmos, V., Lepori, E. V., Ahsan, H., Parvez, F., 2012. Arsenic exposure in Latin America: biomarkers, risk assessments and related health effects. Sci. Total Environ. 429, 76–91. https://doi.org/10.1016/j.scitotenv.2011.08.051.
Meixner, A., Sarchi, C., Lucassen, F., Becchio, R., Caffe, P.J., Lindsay, J., Rosner, M., Kasemann, S.A., 2020. Lithium concentrations and isotope signatures of Palaeozoic basement rocks and Cenozoic volcanic rocks from the Central andean arc and back-arc. Miner. Deposita 55, 1071–1084. https://doi.org/10.1007/s00126-019-00915-2.
Millot, R., Vigier, N., Gaillardet, J., 2010. Behaviour of lithium and its isotopes during weathering in the mackenzie basin, Canada. Geochem. Cosmochim. Acta 74, 3897–3912. https://doi.org/10.1016/j.gca.2010.04.025.
Moon, J.W., 2024. The mineral industry of China. US Geol. Surv. 9, 1–9.46.
Morales-Simfors, N., Bundschuh, J., Herath, I., Inguaggiato, C., Caselli, A.T., Tapia, J., Choquehuayta, F.E.A., Armienta, M.A., Ormachea, M., Joseph, E., López, D.L., 2020. Arsenic in Latin America: a critical overview on the geochemistry of arsenic originating from geothermal features and volcanic emissions for solving its environmental consequences. Sci. Total Environ. 716, 135564. https://doi.org/10.1016/j.scitotenv.2019.135564.
Morteani, G., Möller, P., Dulski, P., Preinfalk, C., 2014. Major, trace element and stable isotope composition of water and muds precipitated from the hot springs of Bolivia: are the waters of the spring's potential ore forming fluids? Geochemistry 74, 49–62. https://doi.org/10.1016/j.chemer.2013.06.002.
Muller, E., Gaucher, E.C., Durlet, C., Moquet, J.S., Moreira, M., Rouchon, V., Louvat, P., Bardoux, G., Noirez, S., Bougeault, C., Vennin, E., Gérard, E., Chavez, M., Virgone, A., Ader, M., 2020. The origin of Continental carbonates in Andean salars: a multi-tracer geochemical approach in Laguna pastos grandes (Bolivia). Geochem. Cosmochim. Acta 279, 220–237. https://doi.org/10.1016/j.gca.2020.03.020.
Munk, L.A., Boutt, D., Butler, K., Russo, A., Jenckes, J., Moran, B., Kirshen, A., 2025. Lithium brines: origin, characteristics, and global distribution. Econ. Geol. 120, 575–597. https://doi.org/10.5382/econgeo.5134.
Murray, J., Guzmán, S., Tapia, J., Nordstrom, D.K., 2023. Silicic volcanic rocks, a main regional source of geogenic arsenic in waters: insights from the Altiplano-Puna Plateau, central andes. Chem. Geol. 629, 121473. https://doi.org/10.1016/j.chemgeo.2023.121473.
Ormachea Muñoz, M., Bhattacharya, P., Sracek, O., Ramos Ramos, O., Quintanilla Aguirre, J., Bundschuh, J., Maity, J.P., 2015. Arsenic and other trace elements in thermal springs and in cold waters from drinking water Wells on the Bolivian altiplano. J. South Am. Earth Sci. 60, 10–20. https://doi.org/10.1016/j.jsames.2015.02.006.
Ormachea Muñoz, M., Wern, H., Johnsson, F., Bhattacharya, P., Sracek, O., Thunvik, R., Quintanilla, J., Bundschuh, J., 2013. Geogenic arsenic and other trace elements in the shallow hydrogeologic system of southern poopó basin, Bolivian altiplano. J. Hazard Mater. 262, 924–940. https://doi.org/10.1016/j.jhazmat.2013.06.078.
Palacios, Noelia A., Lezama, Juan R., Erdmann, Eleonora, Flexer, Victoria, 2026. Calculations on chemicals, water, and energy consumption for the evaporitic process for lithium carbonate recovery from brines: a baseline for technology and environmental impact assessment. Ind. Eng. Chem. Res. 65 (9), 4681–4702. https://doi.org/10.1021/acs.iecr.5c05085. https://pubs.acs.org/doi/10.1021/acs.iecr.5c05085. (Accessed 26 February 2026).
Pistiner, J.S., Henderson, G.M., 2003. Lithium-isotope fractionation during Continental weathering processes. Earth Planet Sci. Lett. 214, 327–339. https://doi.org/10.1016/S0012-821X(03)00348-0.
Placzek, C.J., Quade, J., Patchett, P.J., 2011. Isotopic tracers of paleohydrologic change in large Lakes of the Bolivian altiplano. Quat. Res. 75, 231–244. https://doi.org/10.1016/j.yqres.2010.08.004.
Placzek, C.J., Quade, J., Patchett, P.J., 2013. A 130ka reconstruction of rainfall on the Bolivian altiplano. Earth Planet Sci. Lett. 363, 97–108. https://doi.org/10.1016/j.epsl.2012.12.017.
Price, C.J., Strong, P.L., Marr, M.C., Myers, C.B., Murray, F.J., 1996. Developmental toxicity NOAEL and postnatal recovery in rats fed boric acid during Gestation1. Fund. Appl. Toxicol. 32, 179–193. https://doi.org/10.1093/toxsci/32.2.179.
R Core Team, 2023. R: a Language and Environment for Statistical Computing.
Risacher, F., Alonso, H., Salazar, C., 2003. The origin of brines and salts in Chilean salars: a hydrochemical review. Earth Sci. Rev. 63, 249–293. https://doi.org/10.1016/S0012-8252(03)00037-0.
Risacher, F., Fritz, B., 1991a. Quaternary geochemical evolution of the salars of uyuni and coipasa, central altiplano, Bolivia. Chem. Geol. 90, 211–231. https://doi.org/10.1016/0009-2541(91)90101-V.
Risacher, F., Fritz, B., 1991b. Geochemistry of Bolivian salars, lipez, southern altiplano: origin of solutes and brine evolution. Geochem. Cosmochim. Acta 55, 687–705. https://doi.org/10.1016/0016-7037(91)90334-2.
Risacher, F., Fritz, B., 2000. Bromine geochemistry of salar de Uyuni and deeper salt crusts, Central Altiplano, Bolivia. Chem. Geol. 167, 373–392. https://doi.org/10.1016/S0009-2541(99)00251-X.
Risacher, F., Fritz, B., 2009. Origin of salts and brine evolution of Bolivian and Chilean salars. Aquat. Geochem. 15, 123–157. https://doi.org/10.1007/s10498-008-9056-x.
Rissmann, C., Leybourne, M., Benn, C., Christenson, B., 2015. The origin of solutes within the groundwaters of a high andean aquifer. Chem. Geol. 396, 164–181. https://doi.org/10.1016/j.chemgeo.2014.11.029.
Rosner, M., Erzinger, J., Franz, G., Trumbull, R.B., 2003. Slab-derived boron isotope signatures in arc volcanic rocks from the central andes and evidence for boron isotope fractionation during progressive slab dehydration. G-cubed 4. https://doi.org/10.1029/2002GC000438.
Sajkowski, L., Turnbull, R., Blundy, J., Rogers, K., 2025. Experimental assessment of sustainable lithium extraction from geothermal reservoirs. Geothermics 132, 103448. https://doi.org/10.1016/j.geothermics.2025.103448.
Schmitt, A.K., Kasemann, S., Meixner, A., Rhede, D., 2002. Boron in central Andean ignimbrites: implications for crustal boron cycles in an active Continental margin. Chem. Geol. 183, 333–347. https://doi.org/10.1016/S0009-2541(01)00382-5.
Schnurr, W.B.W., Trumbull, R.B., Clavero, J., Hahne, K., Siebel, W., Gardeweg, M., 2007. Twenty-five million years of silicic volcanism in the southern central volcanic zone of the andes: geochemistry and magma genesis of ignimbrites from 25 to 27 °S, 67 to 72 °W. J. Volcanol. Geoth. Res. 166, 17–46. https://doi.org/10.1016/j.jvolgeores.2007.06.005.
Shaw, D.M., Sturchio, N.C., 1992. Boron-lithium relationships in rhyolites and associated thermal waters of young silicic calderas, with comments on incompatible element behaviour. Geochem. Cosmochim. Acta 56, 3723–3731. https://doi.org/10.1016/0016-7037(92)90165-F.
Shinjoe, H., Orihashi, Y., Naranjo, J.A., Hirata, D., Hasenaka, T., Fukuoka, T., Sano, T., Anma, R., 2013. Boron and other trace element constraints on the slab-derived component in Quaternary volcanic rocks from the southern volcanic zone of the andes. Geochem. J. 47, 185–199. https://doi.org/10.2343/geochemj.2.0241.
Smedley, P.L., Kinniburgh, D.G., 2002. A review of the source, behaviour and distribution of arsenic in natural waters. Appl. Geochem. 17, 517–568. https://doi.org/10.1016/S0883-2927(02)00018-5.
Stern, C.R., 2004. Active Andean volcanism: its geologic and tectonic setting. Rev. Geol. Chile 31, 161–206. https://doi.org/10.4067/S0716-02082004000200001.
Tapia, J., Murray, J., Ormachea, M., Tirado, N., Nordstrom, D.K., 2019. Origin, distribution, and geochemistry of arsenic in the altiplano-puna Plateau of Argentina, Bolivia, Chile, and Perú. Sci. Total Environ. 678, 309–325. https://doi.org/10.1016/j.scitotenv.2019.04.084.

Tirado, N., Mamani, J., De Loma, J., Ascui, F., Broberg, K., Gardon, J., 2024. Genotoxicity in humans exposed to arsenic, lithium, and boron in drinking water in the Bolivian andes—A cross sectional study. Environ. Mol. Mutagen. 65, 121–128. https://doi.org/10.1002/em.22587.

Vera, M.L., Torres, W.R., Galli, C.I., Chagnes, A., Flexer, V., 2023. Environmental impact of direct lithium extraction from brines. Nat. Rev. Earth Environ. 4, 149–165. https://doi.org/10.1038/s43017-022-00387-5.

Weir, R.J., Fisher, R.S., 1972. Toxicologic studies on borax and boric acid. Toxicol. Appl. Pharmacol. 23, 351–364. https://doi.org/10.1016/0041-008X(72)90037-3.

WHO, 2003. Arsenic, Drinking-water and Health Risks Substitution in Arsenic Mitigation : a Discussion Paper. https://www.who.int/publications/m/item/arsenic-drinking-water-and-health-risks-substitution-in-arsenic-mitigation-a-discussion-paper.

Williams, G.D.Z., Barre, J., Louvat, P., Bérail, S., Millot, R., Vengosh, A., 2026. Geochemical controls on the formation of lithium brines in closed-basins of the lithium triangle. Earth Planet Sci. Lett. 679, 119849. https://doi.org/10.1016/j.epsl.2026.119849.

Williams, G.D.Z., Nativ, P., Vengosh, A., 2025a. The role of boron in controlling the pH of lithium brines. Sci. Adv. 11. https://doi.org/10.1126/sciadv.adw3268 eadw3268.

Williams, G.D.Z., Petrović, M., Hill, R.C., Hall, G.A., Vengosh, A., 2025b. The water quality impacts of legacy hard-rock lithium mining and processing. Environ. Sci. Technol. 59, 16492–26505. https://doi.org/10.1021/acs.est.5c13682.

Williams, G.D.Z., Vengosh, A., 2025. Quality of wastewater from lithium-brine mining. Environ. Sci. Technol. Lett. 12, 151–157. https://doi.org/10.1021/acs.estlett.4c01124.

Williams, G.D.Z., Vengosh, A., 2026. Origins of the Mg/Li ratio in closed-basin brines of the lithium triangle: the relative importance of high- and low-temperature water-rock interactions. Earth Sci. Rev. 278, 105516. https://doi.org/10.1016/j.earscirev.2026.105516.

YLB, 2019. Memoria Institucional 2019.

Yuan, X., Hu, Y., Zhao, Y., Li, Q., liu, C., 2021. Contribution of hydrothermal processes to the enrichment of lithium in brines: evidence from water–rock interacting experiments. Aquat. Geochem. 27, 221–239. https://doi.org/10.1007/s10498-021-09395-1.